People's Democratic Republic of Algeria
Ministry of Higher Education and Scientific Research

University M'Hamed BOUGARA – Boumerdes

Institute of Electrical and Electronic Engineering

Department of Electronics

Final Year Project Report Presented in Partial Fulfilment of the Requirements for the Degree of

'MASTER'

In **Telecommunication**
Option: **Telecommunications**

Title:

Analysis of a Reconfigurable Multi-Band Monopole Antenna

Presented By:

- **GHARBI Abdelhamid**
- **BELGACEM Abdelmalek**

Supervisor:

Dr M. DEHMAS

Registration Number:……/2021

Dedication

We would like to dedicate this work to our dear families.

Acknowledgment

First and foremost, praises and thanks are to Allah Almighty for his blessings and his guidance which enables us to complete our finale year report.

We would like to express our deep and sincere gratitude to our supervisor **Dr. Mokrane DEHMAS** for his guidance and unwavering support during this work. We have been tremendously moved by his enthusiasm, vision, integrity and motivation. It was a true honor working with him.

We would like to express our gratitude to **Pr. A. AZRAR** for his help and assistance for the accomplishment of this work.

Special thanks go to **Dr. K. DJAFRI** and **Dr. F. MOUHOUCHE** for their precious help and support in the implementation and measurements.

Last but not least, we are infinitely grateful to our family members, particularly our parents for their endless encouragement.

List of figures

List of tables

List of Abbreviations

2G	Second generation
AMPS	Advanced Mobile Phone System
DC	Direct Current
DCS	Digital Cellular System
GPS	Global positioning system
GSM	Global system for mobile communication
IMT	International mobile telecommunication
ISM	Industrial, Scientific and Medical
MIMO	Multiple-input multiple-output
PCB	Printed Circuit Board
PCS	Personal Communications service
PIN diode	Positive-intrinsic-negative diode
Radar	Radio Detection and Ranging
RFMEMS	Radiofrequency micro-electromechanical system
TM	Transverse Magnetic
UMTS	Universal mobile telecommunication systems
VSWR	Voltage standing wave ratio
W-CDMA	Wideband Code Division Multiple Access
Wi-fi	Wireless Fidelity
WLAN	Wireless Local Area Network

Table of contents

Abstract

This work deals with analysis of a monopole and frequency reconfigurable E-shape patch antenna using FR-4 substrate.

The first step concerns modification of a published reconfigurable antenna due to difference in physical properties of the used substrate and the one at our disposal. These appropriate modifications have been performed on the antenna dimensions and on the stripline width so that the modified structure fits the original antenna band characteristics.

In the second step, which concerns the main contribution of this work, a parametric analysis of the first structure focusing on the slot positions is achieved. The analysis ended up with nine (9) antenna geometrical configurations each one operating in four (4) reconfigurable modes. These antennas fulfill and satisfy various applications.

One of these antenna configurations -operating in one single-band and three dual band reconfigurable modes- has been considered for further analysis.

Prototypes of the modified original antenna as well as the one selected in the second part have been fabricated and their reflection coefficients in open switch positions mode measured where good agreements with simulated results have been obtained.

General Introduction

Antennas are necessary and critical components of communication and radar systems. By the advent of microstrip technology, a great effort has been directed towards development of better microstrip antenna structures that allow better performance to be used in various applications of telecommunication systems. The microstrip antenna is a very good common element in telecommunication since it provides a wide variety of designs, can be planar or conformal, and can be fed using different methods [1] Currently, the use of microstrip antennas has grown due to the advantages of these kinds of structures.

It is well known that microstrip antennas have several shapes and can perform in different ways depending on the application. With the rapid growth of wireless mobile communication, future technologies need very small wide band and multi band antennas to avoid using many antennas [2], but sometimes their inability to adjust to new operating scenarios can limit system performance.

Making antennas reconfigurable so that their behavior can adapt with changing system requirements or environmental conditions can ameliorate or eliminate these restrictions and provide additional levels of functionality for any system [3].

Reconfigurability, when used in the context of antennas, is the capacity to change an individual radiator's fundamental operating characteristics through electrical, mechanical, or other means [4].

Ideally, reconfigurable antennas should be able to alter their operating frequencies, impedance bandwidths, polarizations, and radiation patterns independently to accommodate changing operating requirements. However, the development of these antennas generates significant challenges to both antenna and system designers. These challenges lie not only in obtaining the desired levels of antenna functionality but also in integrating this functionality into complete systems to arrive at efficient and cost-effective solutions. As in many cases of technology development, most of the system cost will come not from the antenna but the surrounding technologies that enable reconfigurability [3].

Our work examines a frequency-reconfigurable planar E-shape patch antenna originally published in [5]. Due to differences in the properties of the FR-4 substrate used in [5] and the one available at our

disposal, necessary adjustments to the effective resonant lengths and stripline width have been made so that the modified structure fits the original antenna band characteristics and to be matched with the 50-Ω cable.

The second stage is to do a parametric analysis of the initial structure in terms of slot locations, which is the main work contribution. Nine (9) different antenna geometrical configurations have been considered, each with four (4) different reconfigurable modes.

Prototypes of the modified original antenna as well as the one selected in the second part have been fabricated and their reflection coefficients at open switch positions measured. Good agreements with simulated results have been obtained.

This report is divided into three main parts:

The first chapter provides an introduction to microstrip patch antennas, including a general description, fundamental operating principles, feeding methodology, advantages and disadvantages, as well as multiband antennas and reconfigurability techniques.

In chapter two, the "CST" program was used to analyze the modified original antenna. The simulated results include reflection coefficient, current distribution as well as the radiation patterns at the four (4) modes of operation of the reconfigurable antenna.

Chapter three describes the parametric analysis of the first structure concerning slot locations, and the study concerned nine (9) antenna geometrical structures, each operating in four (4) reconfigurable modes. Further analysis was carried out on a selected antenna configuration.

Finally, a conclusion along with suggestions for further scope are given at the end of the report.

Chapter One

Generalities on Microstrip Patch Antennas

1.1 Introduction

An antenna is a transducer designed to transmit or receive electromagnetic waves. Microstrip antennas have several advantages over conventional microwave antenna and therefore are widely used in many practical applications [6]. Microstrip antenna in its simplest configuration is shown in Fig1.1. It consists of a radiating patch on one side of dielectric substrate ($\varepsilon_r \leq 10$), which has a ground plane on other side.

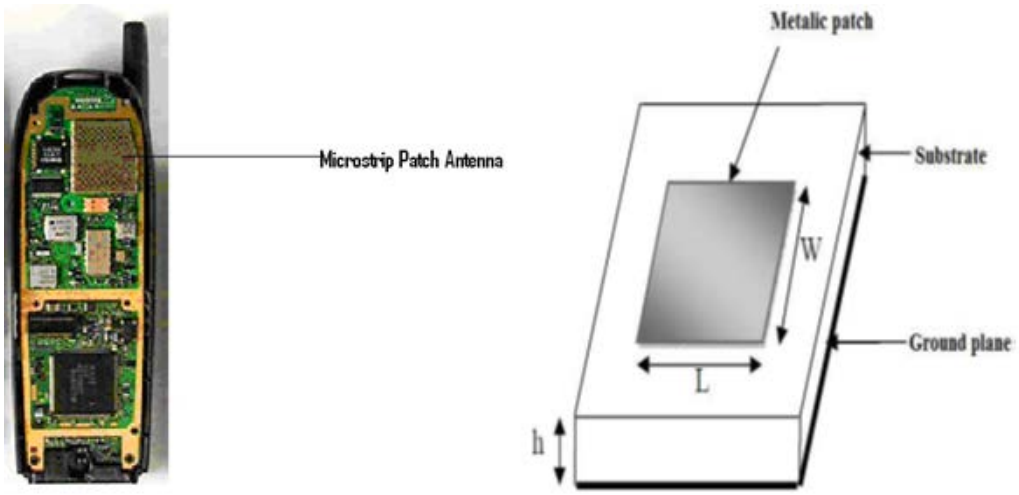

Figure 1.1 A Microstrip patch antenna [7] and its location on phone

Microstrip antennas are characterized by a larger number of physical parameters than conventional microwave antennas. They can be designed to have many geometrical shapes and dimensions [8].

1.2 Physical description

A microstrip antenna is a resonant style radiator. It consists of a radiating patch on one side of a dielectric substrate with a ground plane on the other side as shown in figure 1.1. Generally, the patch consists of a conducting material such as copper which is the source of radiation where electromagnetic energy fringes off the edges of the patch and into the substrate. The length L of the patch is usually $0.333\ \lambda 0 \leq L \leq 0.5\ \lambda 0$ ($\lambda 0$ is the free space wavelength). The patch is selected to be very thin such that $t << \lambda 0$ (t is the patch thickness) [9]. The ones that are most desirable for antenna performance are thick substrates whose dielectric is in the lower end of the range because they provide better efficiency and larger bandwidth [10]. Often microstrip antennas are also referred to as patch antennas. The radiating elements and the feed lines are usually photo-etched on the dielectric substrate. The radiating patch may be square, rectangular, thin strip (dipole), circular, elliptical, triangular any other configuration. Some of them are illustrated in figure 1.2. Microstrip antenna is characterized by its length, Width, input impedance, Polarization, Gain and radiation pattern [8]:

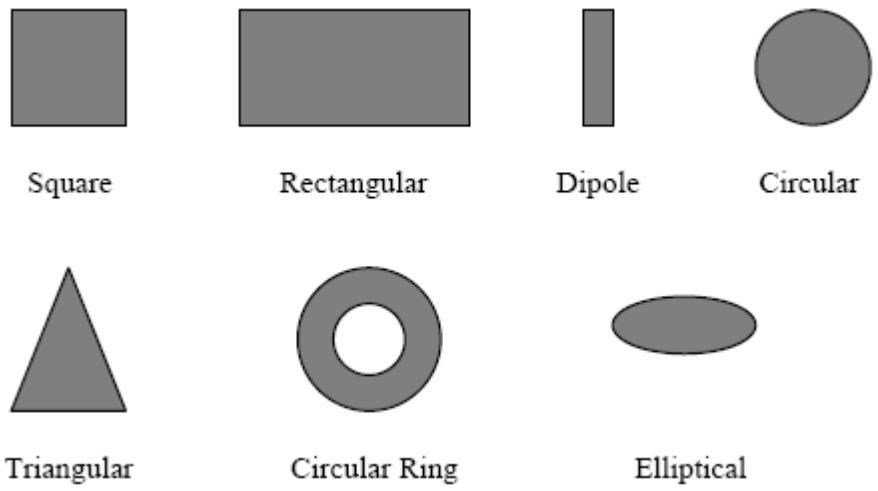

Figure 1.2 Representative shapes of microstrip patch elements.

1.3 Advantages and disadvantages

Microstrip antennas present several advantages compared to conventional microwave antennas and cover the broad frequency range laying from 100 MHz to 100 GHz. Some of the principal advantages of microstrip antenna compared to conventional microwave antennas are:

- Lightweight, low volume and thin profile configuration.
- Low fabrication cost, readily open to mass production.
- Feed lines and matching networks can be fabricated simultaneously with the antenna structure.
- Linear and circular polarizations are possible with simple feed.
- Possibility of dual and triple-frequency operations.
- No cavity backing is required [11].

However, microstrip antennas also have some limitations compared to conventional microwave antenna such as:

- Narrow bandwidth and associated tolerance problems.
- Low gain.
- Low power-handling capability [11].

1.4 Basic Principle of operation

Figure 1.3 shows a patch antenna in its basic form: a flat plate over a ground plane (usually a PC board). The center conductor of a coaxial cable serves as the feed probe to couple electromagnetic energy in and/or out of the patch. The electric field distribution of a rectangular patch excited in its fundamental mode is also indicated [12].

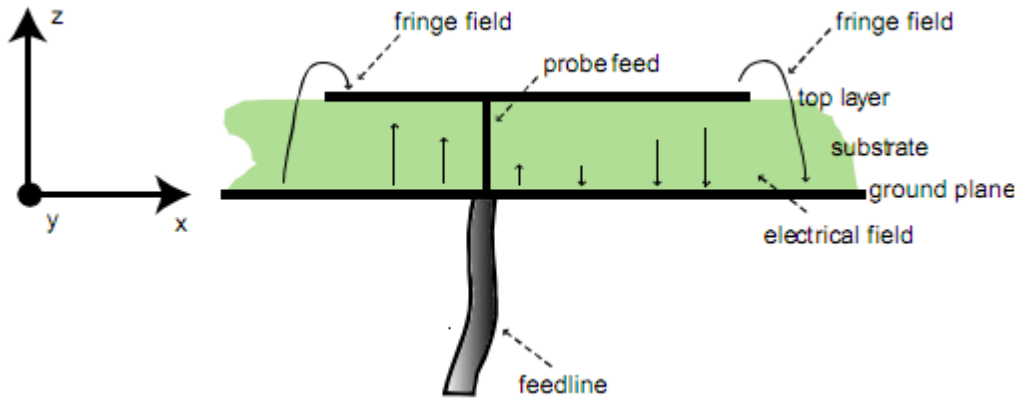

Figure1.3 A Side view of Microstrip Patch Antenna [13].

The electric field is zero at the center of the patch, maximum (positive) at one side, and minimum (negative) on the opposite side. It should be mentioned that the minimum and maximum continuously change side according to the instantaneous phase of the applied signal.

The electric field does not stop suddenly at the patch's periphery as in a cavity; rather, the fields extend the outer periphery to some degree. These field extensions are known as fringing fields and cause the patch to radiate. Some popular analytic modeling techniques for patch antennas are based on this leaky-cavity concept. Therefore, the fundamental mode of a rectangular patch is often denoted using cavity theory as the TM10 mode. [9].

1.5 Application of Microstrip Antennas

The advantages of microstrip antennas make them suitable for numerous applications. Telemetry and communications antennas on missiles need to be thin and conformal and are often microstrip type antennas. Radar altimeters use small arrays of microstrip radiators. Other aircraft-related applications include antennas for telephone and satellite communications. Microstrip arrays have been used for satellite imaging systems.

Patch antennas have been used on communication links between ships or buoys and satellites.

Smart weapon systems use microstrip antennas because of their thin profile. Pagers, the global system for mobile communication (GSM) and the global positioning system (GPS) are major users of microstrip antennas. Some microstrip antenna applications are listed in Table 1.1

Table 1.1 Typical Applications of Microstrip Antennas [14].

System	Application
Aircraft and ship antennas	Communication and navigation, altimeters, blind landing systems
Missiles	Radar, proximity fuses, and telemetry
Satellite communications	Domestic direct broadcast TV, vehicle-based antennas, communication
Mobile radio	Pagers and hand telephones, man pack systems, mobile vehicle
Remote sensing	Large lightweight apertures
Biomedical	Applicators in microwave hyperthermia

1.6 Feeding Methods

Feeding of a microstrip patch antennas can be achieved using a variety of methods.

These methods can be classified into two categories: contacting and non-contacting. In the contacting method, the power is fed directly to the radiating patch using a connecting element such as a microstrip line. In the non-contacting scheme, electromagnetic field coupling is used to transfer power between the microstrip line and the radiating patch. The four most popular feed techniques are [13]:

- Contacting schemes: Microstrip line (edge feed, inset feed), coaxial probe
- Non-contacting schemes: Aperture coupling, proximity coupling

1.6.1 Coaxial Probe Feed

The coaxial or probe feed arrangement is shown in Figure 1.4. The center conductor of the coaxial connector is soldered to the patch. The main advantage of this feed is that it can be placed at any desired location inside the patch to match with its input impedance, but a major disadvantage is the narrow bandwidth and is difficult to model since a hole has to be drilled in the substrate and the connector extends outside the ground plane [14].

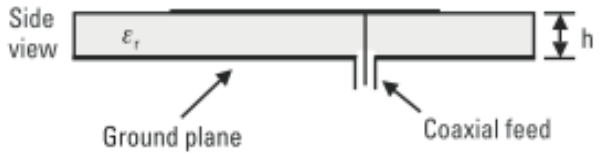

Figure 1.4 Coaxial Feeding of Microstrip Antenna [14].

1.6.2 Microstrip line feed

In this type of feed, a Microstrip line is connected directly to the edge of the patch, and it can be etched on the same substrate of the patch antenna to form a planar structure.

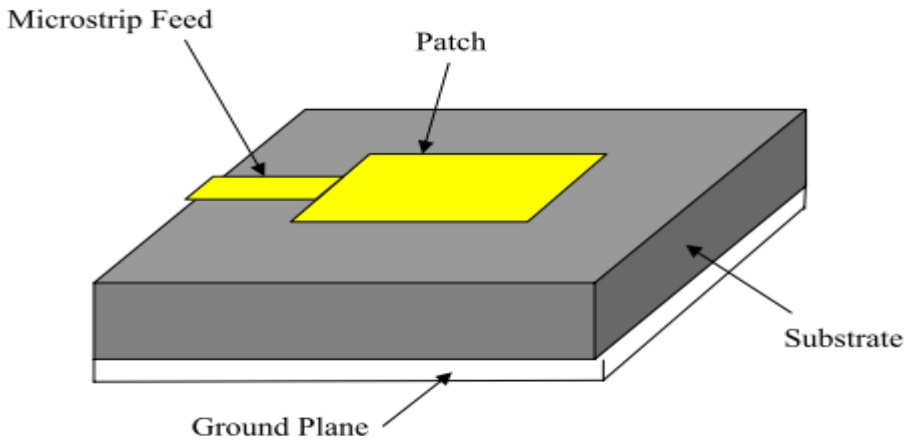

Figure 1.5 Micro-strip line feed [10]

1.6.3 Aperture coupled feed

In this type of feed technique, the radiating patch and the Microstrip feed line are separated by the ground plane. Coupling between the patch and the feed line is made through an aperture in the ground plane as shown in the figure 1.6 [9]. Here separate laminates are used for the feed network and the patch antenna. The laminates are separated by a ground plane and coupling between the feed, in this case a Microstrip line and the patch antenna is achieved via a small slot in the ground-plane. The feed-line is terminated either with an open circuit or a short circuit stub. Aperture-coupled Microstrip patch antennas are probably the most utilized Microstrip patches in today's global market [7].

The major disadvantage of this feed technique is that it is difficult to fabricate due to multiple layers, which also increases the antenna thickness [9].

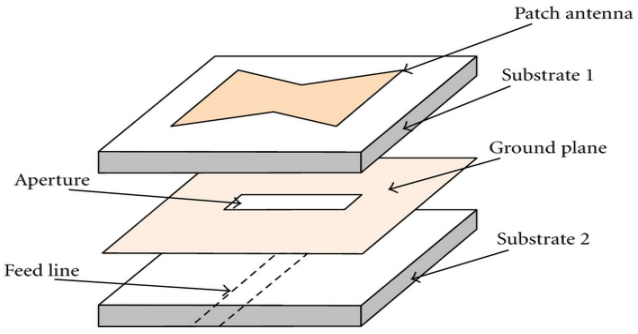

Figure 1.6 Aperture coupled feeding of Microstrip Antenna [15].

1.7 Antenna Parameters

All the antennas have similar criterion to be held in the study, comparison, discussion and analysis. A good antenna should have suitable parameters to classified as successful antenna, some of these parameters are listed below:

1.7.1 Input impedance

The input impedance is the impedance presented by an antenna at its terminal, in other words it is the ratio of the voltage to the current at the pair of terminals or ratio of the appropriate components of the electric to magnetic fields at point [16]. The equation (1.1) shows it in a complex form where the real part is input resistance and the imaginary part representing the input reactance.

$$Zin = R_{in} + jX_{in} \quad (1.1)$$

1.7.2 Reflection coefficient

Depending on the impedance of the antenna and the line feeding the antenna, a certain fraction of transmitted power to the antenna reflects from antenna without radiation. This power fraction is usually described as the Reflection coefficient (Γ[dB]) (or sometimes called as mismatch loss) in decibel scale as:

$$\mathbf{\Gamma[dB] = -20 \log_{10} (| \Gamma |)} \quad (1.2)$$

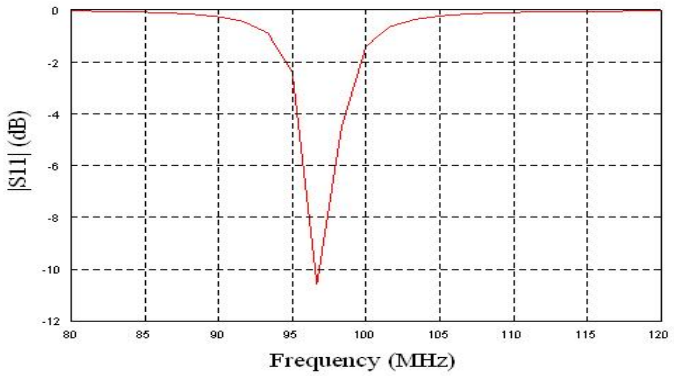

Figure1.7 Reflection coefficient vs frequency

Where Γ is **the reflection coefficient** expressed by:

$$\Gamma = \frac{Z_{IN} - Z_0}{Z_{IN} + Z_0} \quad (1.3)$$

Where **Zin** is the complex input impedance of the antenna and Zo denotes the characteristic impedance of the feed line.

In this work, as an alternative way of describing the reflected power from the antenna, the term **Voltage Standing Wave Ratio** (VSWR) is also used with a formal definition given by:

$$\mathbf{VSWR} = \frac{1+|\Gamma|}{1-|\Gamma|} \quad (1.4)$$

VSWR provides a more quantitative indication about mismatch between the antenna and feeding line impedances that VSWR = 1 indicates perfect matching. Because the complex impedance of antenna is a function of frequency, both Reflection coefficient and VSWR depend on the operating frequency. Thus, if the antenna operates at a given frequency bandwidth, the impedance of the antenna should satisfy application-specific criterion such as VSWR≤ 2 or equivalently Γ ≤ -10 dB at all frequencies within the bandwidth **Zo** of the assumed coaxial cable is 50 Ohms. [12]

1.7.3 Bandwidth

It is defined as "The range of usable frequencies within which the performance of the antenna, with respect to some characteristic, conforms to a specified standard" as it is shown by the figure:

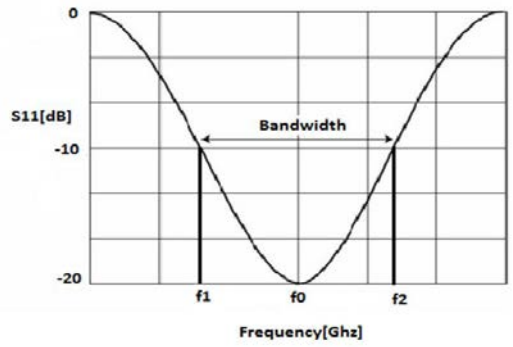

Figure 1.8 Graphical determination of the frequency bandwidth

The percent bandwidth is expressed as:

$$BW = \frac{f2 - f1}{f0} \times 100 \quad (1.5)$$

1.7.4 Radiation pattern

It is defined as "a mathematical function or a graphical representation of the radiation properties of the antenna as a function of space coordinates" [10]. In most cases, the radiation pattern is determined only in the far region and is represented as function of directional coordinates. Radiation properties include power flux density, radiation intensity, field strength, directivity phase and polarization.

1.7.5 Directivity

It is the ratio of the radiation intensity in a given direction from the antenna to the radiation intensity in all directions. The average intensity is equal to the total power radiated by the antenna divided by radiated intensity of isotropic source**.** If the direction is not specified, the direction of maximum radiation intensity is implied. Stated more simply, the directivity of a non-isotropic source is equal to the ratio of its radiation intensity in a given direction over that of an isotropic source. In mathematical form it can be written as:

$$D= \frac{U}{U0} =\frac{4\Pi\, U}{Prad} \qquad (1.6)$$

Where **U0** is radiation intensity of the isotropic source

1.7.6 Polarization

This is the polarization of the wave radiated by the antenna in that particular direction. This is usually dependent on the feeding technique. When the direction is not specified, it is in the direction of maximum radiation [17].

widely used polarization types. We have three types of polarization:

- Linear polarization
- Circular polarization
- Elliptical polarization

1.7.7 Gain

The gain of an antenna is defined as the ratio of the power intensity radiated by the antenna in a given direction (usually in spherical coordinate angles θ and φ) divided by the intensity radiated by a lossless isotropic antenna, which radiates the power at all angles equally.

In a mathematical form, it can be formulated as:

$$Gain=G(\theta.\phi) = 4\pi\frac{U(\theta.\phi)}{P_{in}} \qquad (1.7)$$

or,

$$Gain(\theta.\phi) = e\ D(\theta.\phi) \qquad (1.8)$$

Where e is the efficiency, $e = P_{rad} / P_{in}$

1.8 Multiband Microstrip Patch Antenna

Earlier, mobile Systems were designed to operate for one of the frequency bands of 2G (second generation) systems, which are Digital Cellular System (DCS), Personal Communications Service (PCS) and Global System for Mobile Communications (GSM) networks. Currently, many mobile communication systems use several frequency bands such as GSM 900/1800/1900 bands (890-960 MHz and 1710-1990 MHz); Universal Mobile Telecommunication Systems (UMTS) and UMTS 3G expansion bands (1900-2200 MHz and 2500-2700 MHz); and Wi-Fi (Wireless Fidelity)/Wireless Local Area Networks (WLAN) bands (2400-2500 MHz and 5100-5800 MHz) where the list of frequently used frequency bands is given in Table 1.1 [18].

Conventionally, because a single antenna cannot operate at all of these frequency bands of mobile communication, multiple different antennas covering these bands separately should be used. However, usage of many antennas is usually limited by the volume and cost constraints of the applications. Therefore, multiband antennas are essential to provide multifunctional operations for mobile communication [19].

Table 1.2 Frequency bands for mobile communication applications

Wireless Application	**Alternate Description(s)**	**Frequency Band (MHz)**
GSM 850	AMPS (Advanced Mobile Phone System)	824-894
GSM 900		890-960
GSM 1800	DCS 1800	1710-1885
GSM 1900	W-CDMA (Wideband Code Division Multiple Access); IMT 2000 (International Mobile Telecommunication)	1885-2200
Wi-Fi/WLAN (IEEE 802.11 b/g/n)	ISM 2450 (Industrial, Scientific and Medical)	2400-2484
Wi-Fi/WLAN (IEEE 802.11 y)		3650-3700

1.9 Multiband techniques

In order to realize multiband operation, a wide variety of antenna types, which uses different multiband techniques, are used. The most popular technique for obtaining multiband antenna system is the usage of multiple resonant structures. Here, two or more resonant structures, which are closely located in space or even co-located with a single feed, are used. This is illustrated in Fig.1.9 (a) for dual-band applications that the antennas in both cases have operation center frequencies f_1 and f_2. They are typical examples for corporate feed that two resonant structures are excited simultaneously. [20]. The multiple resonant structure technique is also frequently used in mobile communication systems to achieve multiband mobile antennas. For example, in dual frequency antenna systems for handsets are proposed. The designed structures are the combination of monopole and helical antennas as shown in Fig. 1.9 (b) that multiple resonances at two different frequencies are acquired for dual-band operation at GSM 900 and 1800 bands [19].

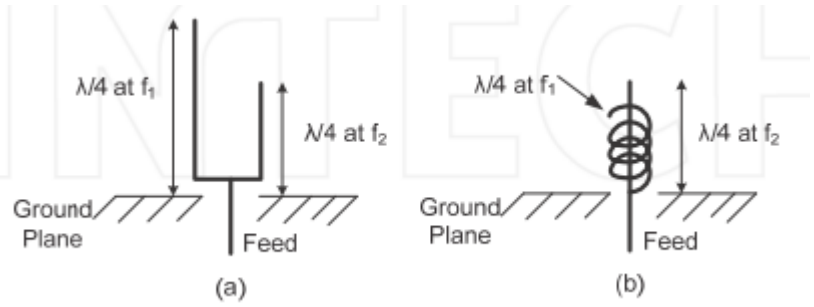

Figure 1.9(a) Two monopole antennas for dual-band operation **(b)** A helical antenna resonate at the frequency f_1 and a monopole antenna resonating at the frequency f_2 for dual-band operation. [21].

1.10 Antenna reconfigurability

Reconfigurable antennas should be able to alter their operating frequencies, impedance bandwidths, polarizations, and radiation patterns independently to accommodate changing operating requirements. However, the development of these antennas makes significant challenges to both antenna and system designers. These challenges lie not only in obtaining the desired levels of antenna functionality but also in integrating this functionality into complete systems to arrive at efficient and cost-effective solutions. As in many cases of technology development, most of the system cost will come not from the antenna but the surrounding technologies that enable reconfigurability [22].

1.11 Advantages of antenna reconfigurability

The study of reconfigurable antennas has made great progress in recent years, compared with conventional antennas, reconfigurable antennas have more advantages and better prospects, and they are lighter in weight, smaller in dimension and lower in price. Moreover, the reconfigurable antenna can provide diversity feature of operating resonant frequency, polarization, and radiation pattern.

1.12 Switching Techniques

In order to demonstrate the reconfigurable antennas, various effective implementation techniques have been proposed to be used in different wireless systems such as satellite, multiple-input multiple-output (MIMO) and cognitive ratio communications, which are classified as below [23]:

- Electrical reconfiguration;
- Optical reconfiguration;
- Physical reconfiguration;

The most common technique is electrical reconfiguration, which uses active elements such as positive–intrinsic–negative (PIN) diodes, varactors and radiofrequency micro-electromechanical system (RFMEMS) switches.

1.12.1 Electrical Reconfiguration

In this type of reconfiguration method, the antenna characteristics are changed using electronic switching components such as PIN diodes, varactors or MEMS. Using these switches, the antenna structure can be reconfigured, which causes the redistribution of the surface current and alters the antenna's fundamental characteristics in terms of frequency, radiation pattern and polarization [23].

PIN Diodes:

The electrical parameters of the diode equivalent model with forward and reverse biases in the ON and OFF states are illustrated in Figure 1.10. PIN diodes are widely used as the switching components in different wireless systems. [23]

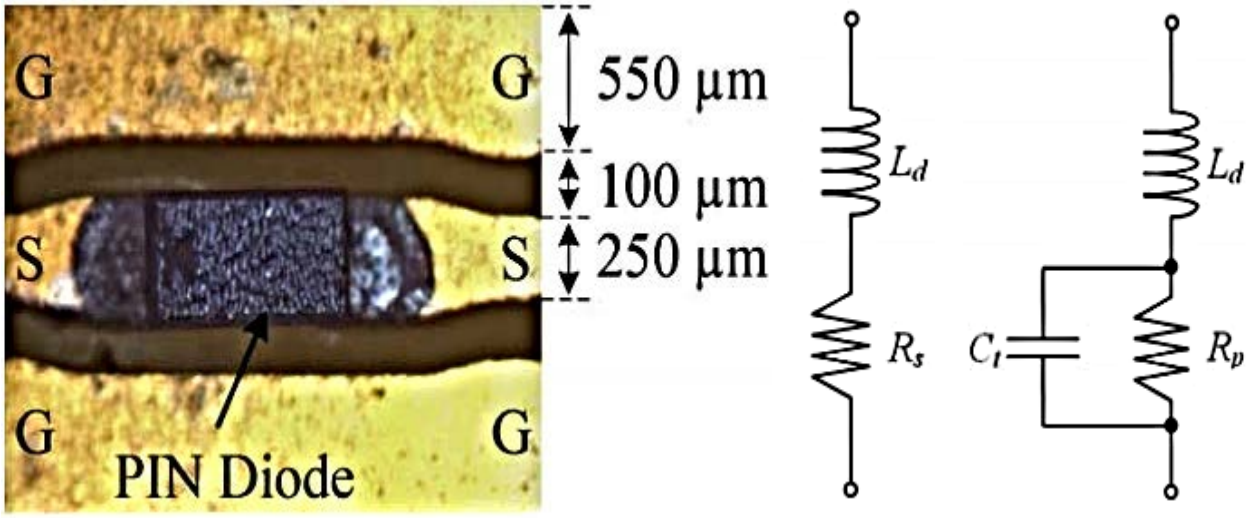

(a) (b) (c)

Figure 1.10 (a) Embedded PIN diode on a prototype, equivalent models for (b) forward and (c) reverse biases (redrawn from [24])

The PIN diode needs a high tuning speed, a high direct current (DC) bias current in the ON-state and a high power-handling capacity. However, it is very reliable and extremely low-cost which makes it a good choice for the reconfiguration technique [23].

Tunable Varactors:

Varactors can also be embeded into the reconfigurable antenna, either on its radiating patch or the feeding line. It requires a direct DC-voltage source. By changing the voltage levels of the varactors, its capacitance changes, which leads to tune the antenna performance. Integrating varactors in reconfigurable designs is a common way to achieve the frequency tuning function [23].

Figure 1.11 Varactor electronic symbol

The varactor is nonlinear with a low dynamic range. It also requires a complex bias circuitry. However, compared with other active elements such as a PIN diode or MEMS, it has a small current flow and continuous tuning characteristics [23].

MEMS:

MEMS switches are devices which operate by the use of mechanical movement to achieve a short or open circuit in RF circuits. MEMS switches can be designed in different configurations based on signal path (series or shunt), the actuation mechanism (electrostatic, thermal or magnetostatic), the type of contact (ohmic or capacitive) and the type of structure (cantilever or bridge).

A comparison of different switching components is provided in Table 1.3. MEMS switches offer some advantages over PIN diodes or varactors, including high isolation and linearity, wide impedance bandwidth, low noise figure and low power losses. However, compared with other RF switches, it requires a high-control voltage and has a slow switching speed and a limited life cycle.

Table 1.3 Comparison of different switch components [23]

Reconfiguration technique	Advantages	Disadvantages
PIN diode	• Very reliable • Extremely low-cost • Common choice for reconfiguration	• High tuning speed • High DC bias in ON-state • High power handling capacity
Varactors	• Small current flow • Continuous tuning • Ease of integration	• Nonlinear • Low dynamic range • Complex bias circuitry
RF MEMS	• High isolation and linearity • Wide impedance bandwidth • Low power losses and low noise figure	• High control voltage • Slow switching speed • Limited life cycle

Chapter Two

Reconfigurable Multi-Band Antenna Analysis

2.1 Introduction

In this chapter, a reconfigurable E-shape multiband antenna fed by a 50-Ω copper annealed microstrip line is analyzed and discussed using the CST electromagnetic simulator. This structure has been considered in [5] where an FR-4 substrate having a relative permittivity of 4.5 and a loss tangent of 0.019 has been used. Due to the difference of the available substrate's parameters (relative permittivity of 4.3 and loss tangent of 0.017), modifications to the effective resonant lengths and to the stripline width so that it will be matched with the 50-Ω cable have been performed.

The work performed in this chapter is a primary step to a second stage achieved in the next chapter which consists of a parametric study which concerns slots positions to end up with a set of reconfigurable antenna configurations fulfilling various applications.

2.2 Antenna geometry

The geometry of the E-shaped investigated antenna [5] is shown in figure 2.1. In [5], they have used a substrate FR-4 material with assumed dielectric permittivity of 4.5, loss tangent of 0.019 and a thickness of 1.6 mm.

As these data are not equal to the available material characteristics, appropriate modifications have been performed on the antenna dimensions and on the stripline width so that the modified structure fits the original antenna band characteristics.

In this work the radiating element is printed on a 1.63 mm FR-4 substrate having a relative permittivity of 4.3 and a loss tangent of 0.017. The antenna is fed with a 50-Ω microstrip line. The antenna is excited using a waveguide port assigned to the feed line and the copper patch thickness is assumed to be a 0.035 mm.

As stated above, the new 50-Ω feed line width is first estimated using the standard transmission line theory [10]. This operation, based on an empirical model in conjunction with a slight adjustment, resulted in a feed line width of w = 3.124 mm.

After that, since the new structure presents shifted band characteristics with respect to the original structure, adjustments of the resonating patch lengths have been performed.

This modification is fundamentally based on the fact for a rectangular microstrip antenna operating at a frequency *f*, the patch resonating length (*L*) is inversely proportional to the square root of the substrate material effective permittivity εeff, that is [10]

$$L\ \alpha\ 1/\sqrt{\varepsilon}eff \tag{2.1}$$

Accordingly, if we assign indices "1" and "2" for the original and the new antenna parameters respectively, then the second antenna resonating dimensions might be primary estimated as follows

$$L_2 = L_1 \times \frac{\sqrt{\varepsilon reff1}}{\sqrt{\varepsilon reff2}} \tag{2.2}$$

That is the patch length should be multiplied by the ratio

$$\frac{\sqrt{\varepsilon reff1}}{\sqrt{\varepsilon reff2}} \approx 1.02 \tag{2.3}$$

Again, this required slight adjustments due to empirical nature of the used models [10].

Two slots of 1 mm are reserved for installation of the switches based on the selected technique. Theses ones are used for switching between the four modes of operation (Table 2.2). In this work, we assume that the switch gap is kept open in OFF state and closed in ON state. This assumption exhibits similar behavior and results when an adequate switching technique is used. However, the latter issue and related analysis focusing on the switching technique is not considered in this work due to the materials, components and circuits behavior at the operating frequencies.

The dimensions of the proposed antenna are shown in table 2.1.

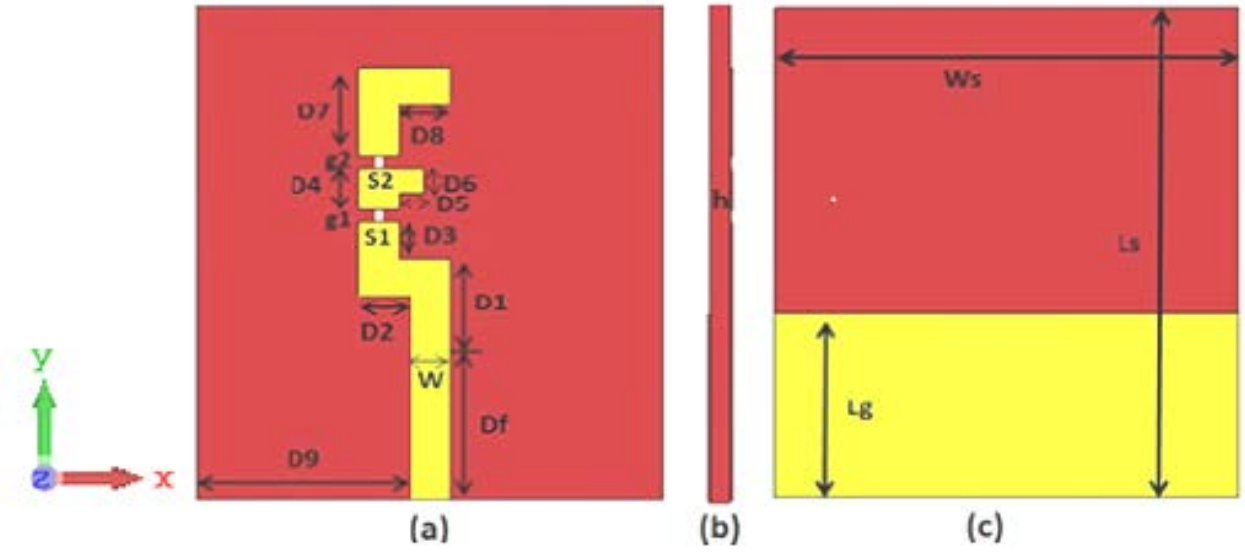

Figure 2.1 E-shaped reconfigurable antenna (a) front view (b) side view (c) rear view

Table 2.1 Proposed antenna dimensions

Length	Values (mm)	Lengths	Values(mm)
D1	6.721	**D9**	16.544
D2	4.136	**W**	3.124
D3	3.102	**g1 = g2**	1
D4	3.5156	**Df**	13.442
D5	2.068	**Ws**	36.19
D6	2.068	**Lg**	15.51
D7	7.4448	**ls**	41.36
D8	4.136	**h**	1.63

2.3 Simulated results

The simulations are carried out using CST Studio, the four modes of operation are summerized in Table 2.2, the analyze of each mode are then performed.

Table 2.2 Switching states and reconfiguration

MODES	S1	S2	FREQUENCY MODE
MODE 1	OFF	OFF	Single-band 5.18 GHz
MODE 2	ON	ON	Dual-band 2.44 GHz & 6.27 GHz
MODE 3	ON	OFF	Single-band 3.77 GHz
MODE 4	OFF	ON	Dual-band 4.77 GHz & 6.23 GHz

2.3.1 Mode 1 (OFF, OFF)

❖ **Reflection coefficient**

When both switches (s1, s2) are turned OFF the antenna operates in mode 1. In this mode, the antenna acts as a single-band antenna (5.18 GHz) having a minimum simulated reflection coefficient of -17.17 dB and a bandwidth of 1.7 GHz (4.6 – 6.3 GHz) as illustrated in Figure 2.2.

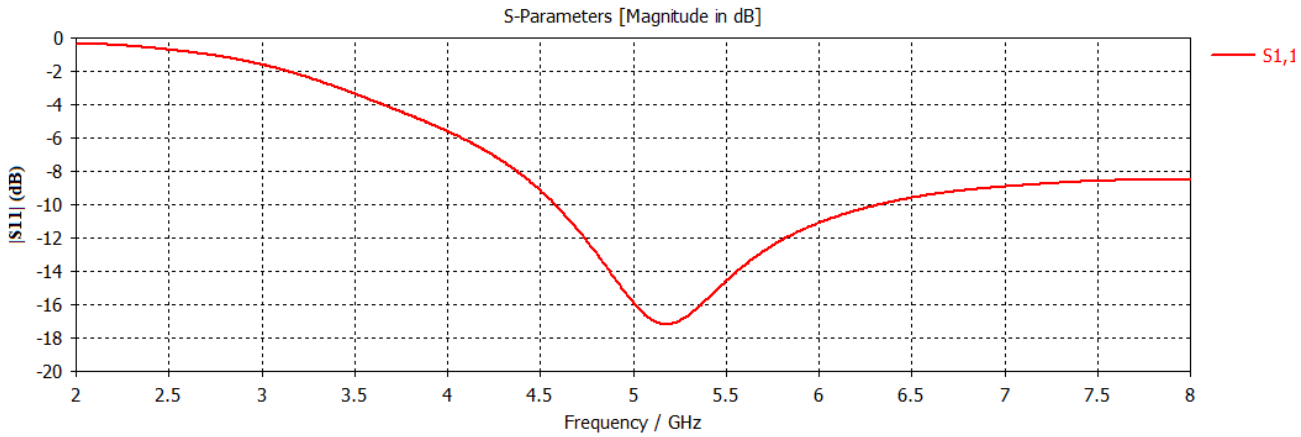

Figure 2.2 Reflection Coefficient at mode 1 (OFF-OFF)

❖ **Current density distribution**

The current density distribution at the resonant frequency of 5.18 GHz at the first mode is illustrated in Figure 2.3. This figure shows that the portion of the patch contributing in the generation of the resonant frequency lies along the feed line before the first slot.

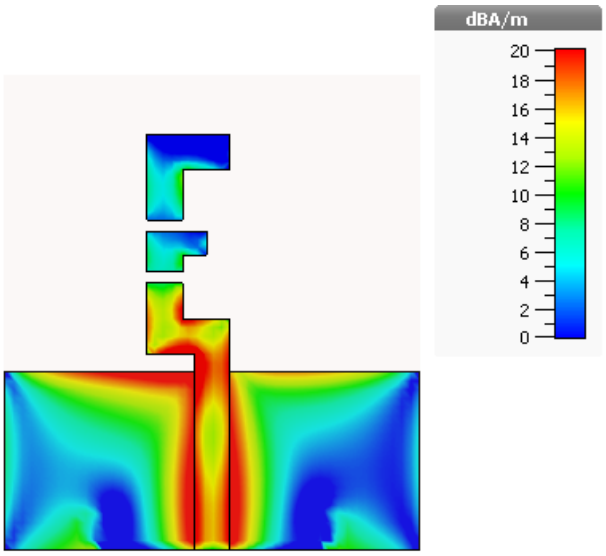

Figure 2.3 Current density distribution at mode 1 (OFF-OFF)
(Single band = 5.18 GHz)

❖ Farfield Radiation Pattern

The simulated farfield radiation patterns of the antenna at the resonant frequency of 5.18 GHz in E-plane (φ=90°) and H-plane (φ= 0°) are illustrated in figure 2.4 and figure 2.5 respectively. In the E-plane, the pattern consists of mainly two lobes in upper and lower hemispheres respectively. The radiation pattern details in both planes are indicated near the graphs.

E-plane(φ=90°)

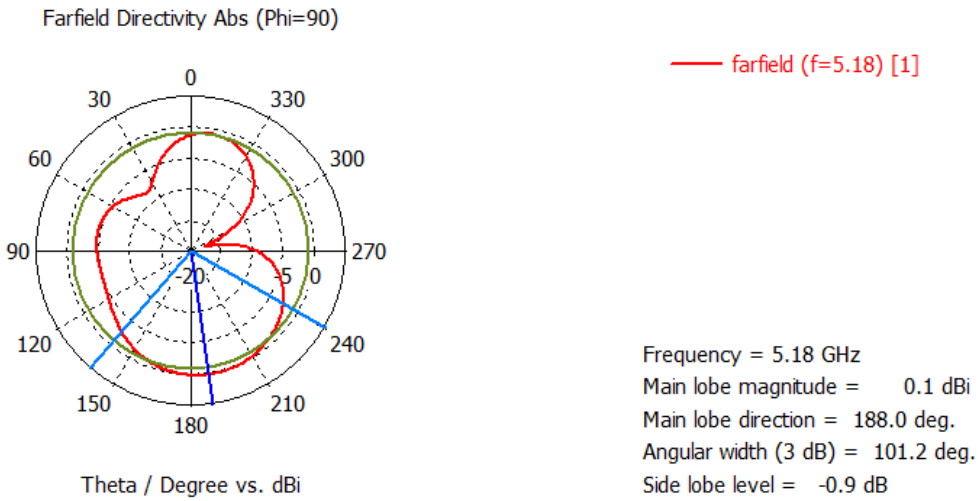

Figure 2.4 E-plane radiation pattern at 5.18 GHz

H-plane (φ= 0°)

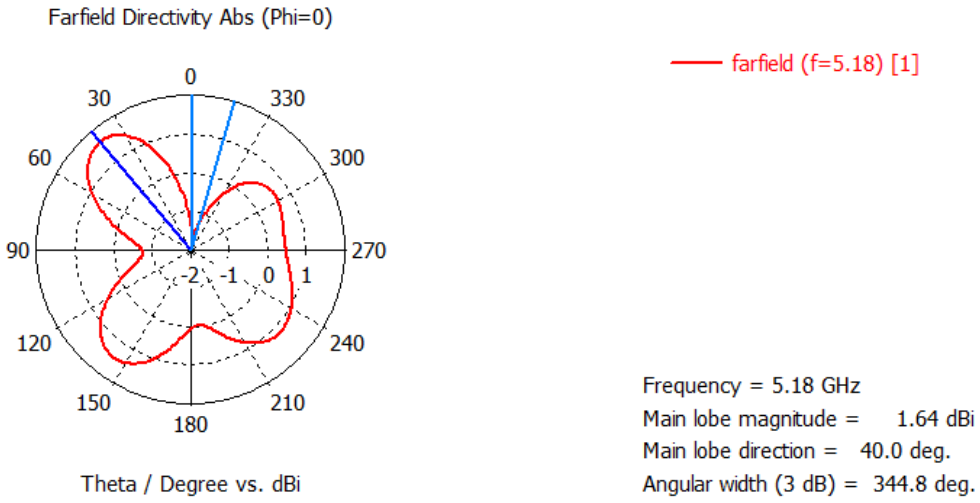

Figure 2.5 H-plane radiation pattern at 5.18 GHz

2.3.2 Mode 2 (ON, ON)

- **Reflection coefficient**

When both switches (s1, s2) are turned ON the antenna operates in mode 2. In this mode, the antenna acts as a dual-band antenna (2.44 & 6.27 GHz) having minimum simulated reflection coefficients of -24.55 dB and -36 dB and bandwidths of 0.5 GHz (2.2 – 2.7 GHz) and 1.1 GHz (5.8 – 6.9 GHz) at 2.44 GHz and 6.27 GHz respectively as illustrated in Figure 2.6.

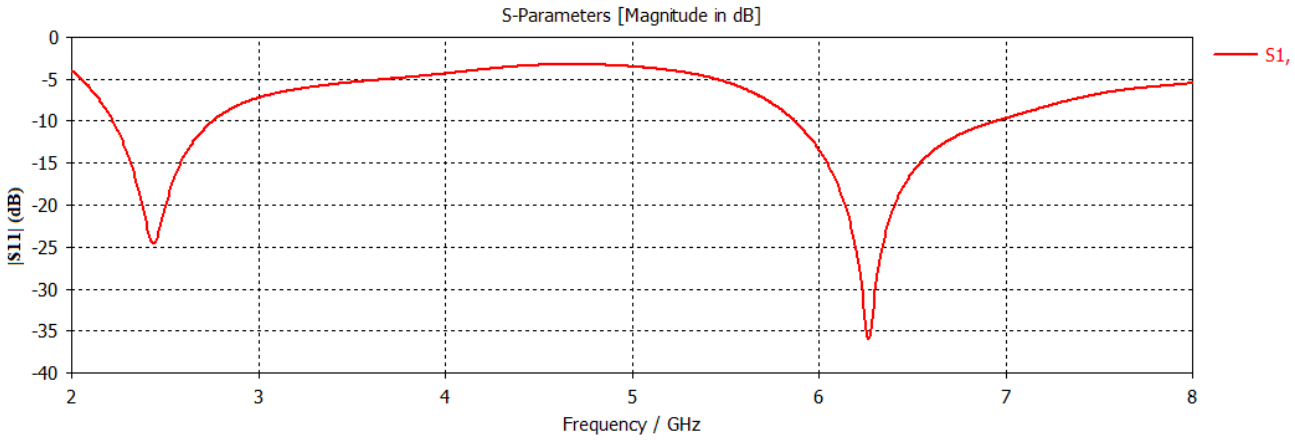

Figure 2.6 Reflection coefficients at mode 2 (ON, ON)

- **Current density distribution**

The current density distribution at the resonant frequencies of 2.44 and 6.27 GHz are illustrated in Figure 2.7. Figure 2.7 (a) shows the current density distribution at frequency 2.44 GHz where the surface current is maximum through the entire length of the radiating element and feed line.

Figure 2.7 (b) illustrates the current density distribution at frequency 6.27 GHz. The surface current is higher along the feed line and the upper vertical segment of the E-shape structure.

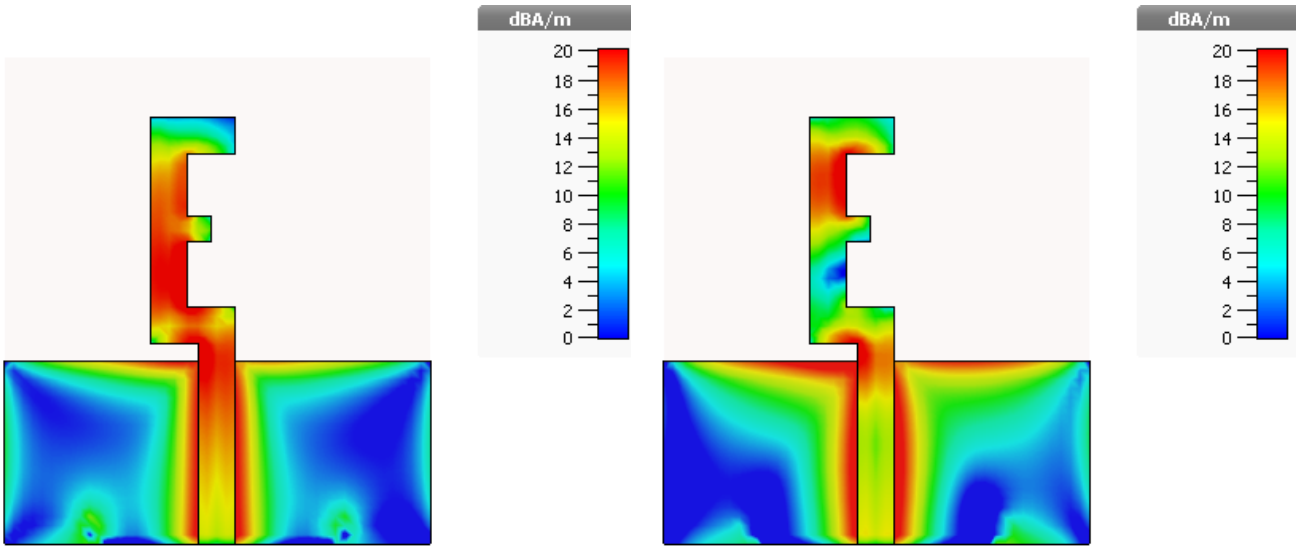

(a) At 2.44 GHz **(b) At 6.27 GHz**

Figure 2.7 Current density distribution at mode 2 (ON-ON)

❖ Farfield Radiation Pattern

The simulated farfield radiation patterns of the antenna at resonance frequencies of 2.44 GHz and 6.27 GHz in E-plane (φ=90°) and H-plane (φ= 0°) are illustrated in figures 2.8-11. Again, it is observed from these figures that the radiation pattern consists of mainly two lobes in the in the upper and lower hemispheres in the directions of θ = 0° and θ =185°. The radiation pattern information at both E and H planes are indicated near the graphs.

At frequency 2.44 GHz

E-plane(φ=90°)

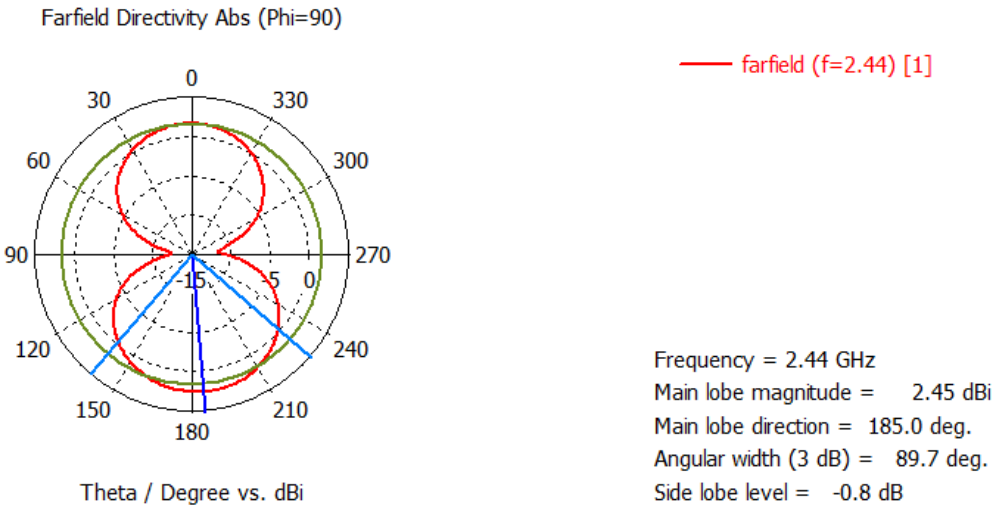

Figure 2.8 E-plane radiation pattern at 2.44 GHz

H-plane (φ= 0°)

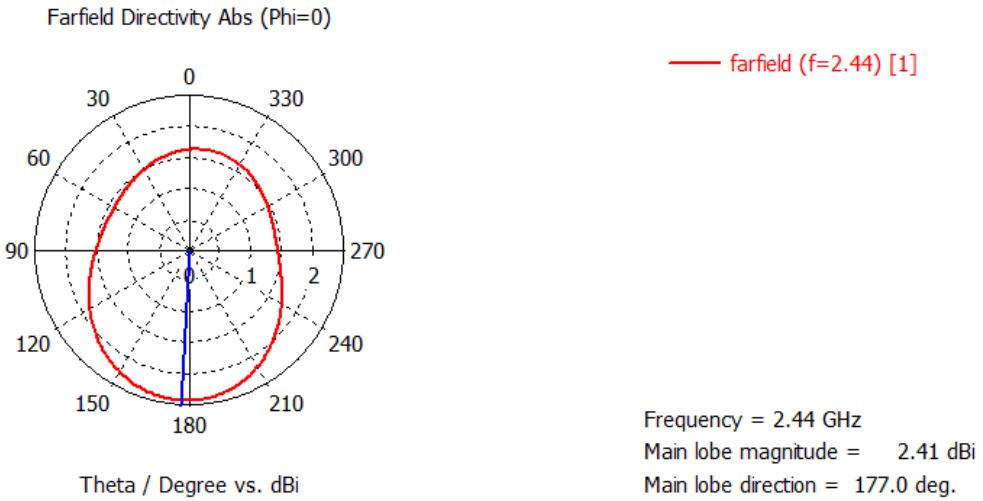

Figure 2.9 H-plane radiation pattern at 2.44 GHz

<u>At frequency 6.27 GHz</u>

E-plane(φ=90°)

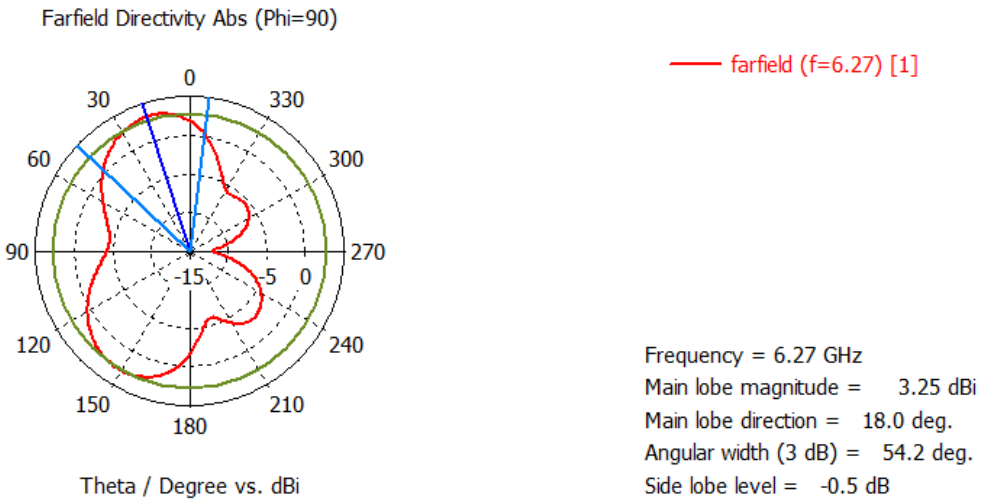

Figure 2.10 E-plane radiation pattern at 6.27 GHz

H-plane (φ= 0°)

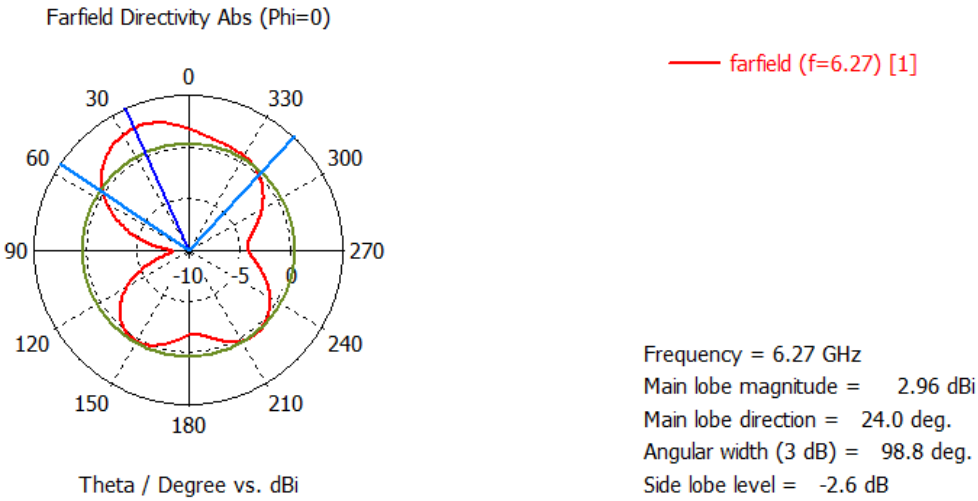

Figure 2.11 H-plane radiation pattern at 6.27 GHz

2.3.3 Mode 3 (ON, OFF)

❖ **Reflection coefficient**

When switch s1 is ON and s2 is OFF, the antenna operates in mode 3. In this mode, the antenna exhibits a single-band operation (3.77 GHz) having a minimum simulated reflection coefficient of -29.02 dB and a bandwidth of 1.5 GHz (3 – 4.5 GHz) as shown in Figure 2.13.

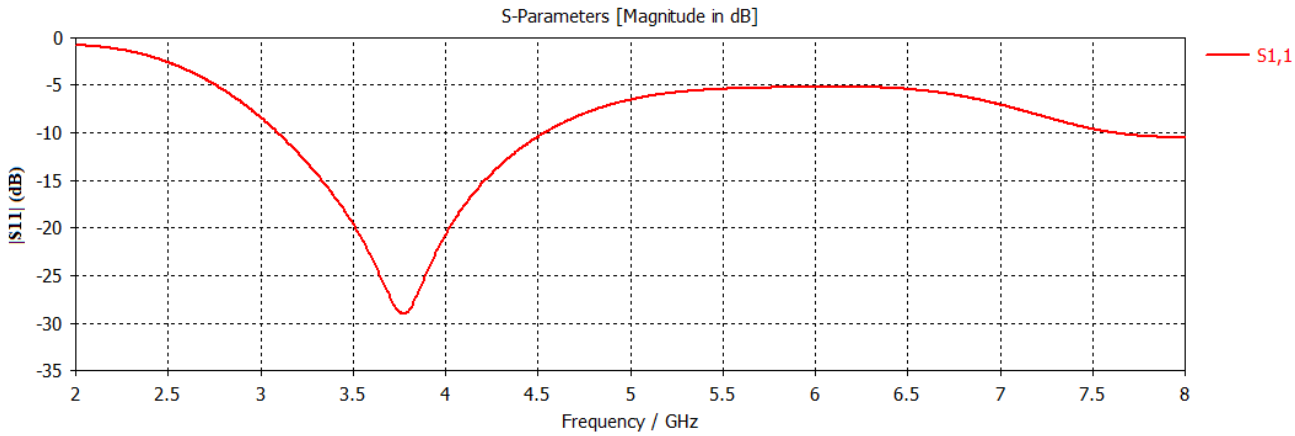

Figure 2.12 Reflection coefficient at mode 3 (ON-OFF)

❖ Current density distribution

Figure 2.13 shows the current density distribution at the resonant frequency of 3.77 GHz. We observe that the surface current is higher through the entire feed line and maximum along the lower segment of the E-shape structure.

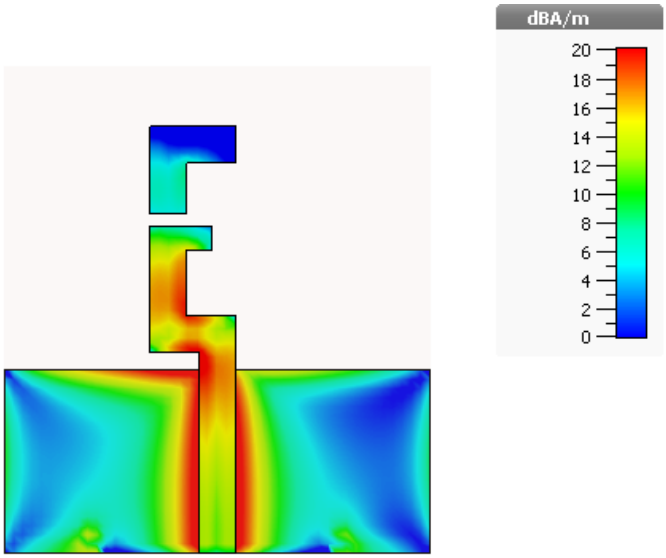

Figure 2.13 Current density distribution at mode 3 (ON-OFF)
(Single band = 3.77 GHz)

❖ Farfield Radiation Pattern

The simulated farfield radiation pattern of the antenna at resonance frequency of 3.77 GHz in E-plane (φ=90°) and H-plane (φ= 0°) are illustrated in figure 2.14 and figure 2.15 respectively. In the E-plane figure, we observe two main lobes, one main lobe in the upper half and a slightly large main

lobe in the lower half. The radiation pattern information at both E and H planes are indicated near the graphs.

E-plane(φ=90°)

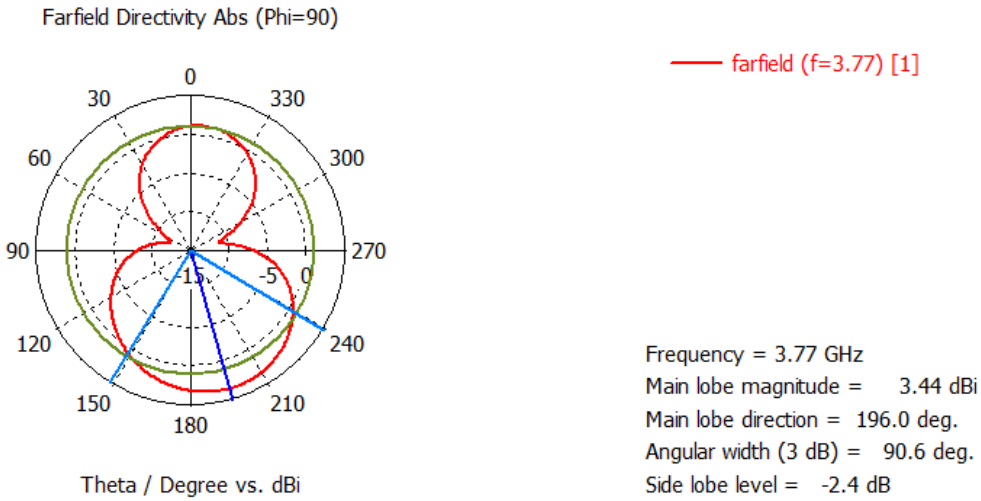

Figure 2.14 E-plane radiation pattern at 3.77 GHz

H-plane (φ= 0°)

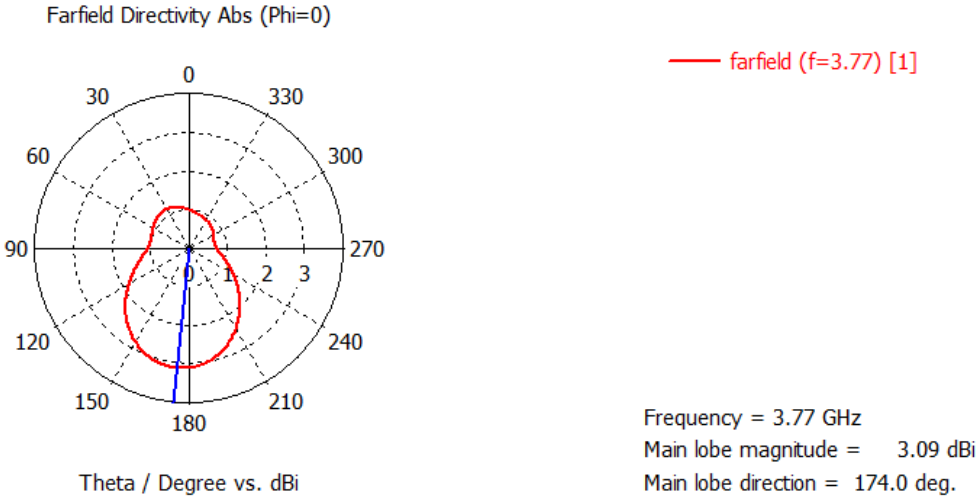

Figure 2.15 H-plane radiation pattern at 3.77 GHz

2.3.4 Mode 4 (OFF,ON)

❖ **Reflection coefficient**

When switch s1 is OFF and s2 is ON, the antenna operates in mode 4. In this mode, the antenna acts as a dual-band antenna (4.77 & 6.23 GHz) having significant minimum levels of simulated

reflection coefficients of -25.69 dB and -29.91 dB and bandwidths of 1.4 GHz (4.15 - 5.55 GHz) and 1.6 GHz (5.55 - 7.15 GHz) respectively as shown in Figure 2.16.

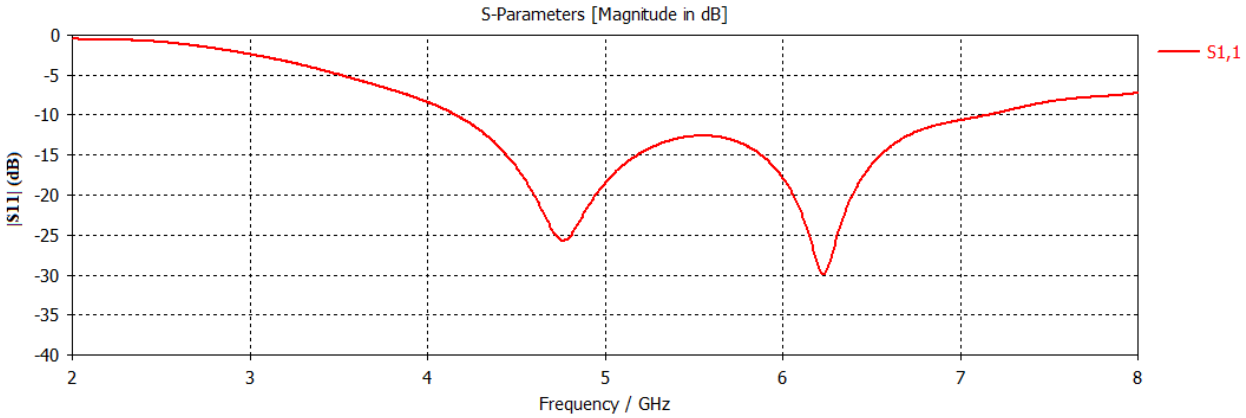

Figure 2.16 Reflection coefficients at mode 4 (OFF-ON)

❖ Current density distribution

The current density distribution at the resonant frequencies of 4.77 and 6.23 GHz are illustrated in Figures 2.17. Figure 2.17 (a) shows the current density distribution at frequency 4.77 GHz where the surface current is maximum along the feed line and the upper part of the E-shape structure. However, we observe that at the frequency of 6.23 the surface current is more concentrated at the upper E-shape portion GHz as illustrated in Figure 2.17 (b).

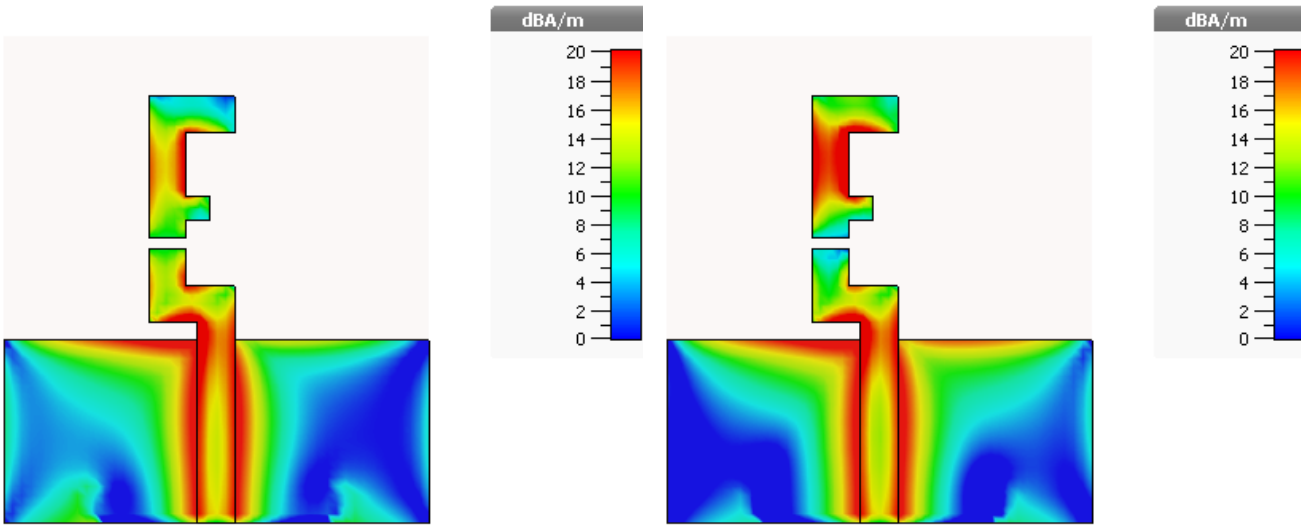

(a) At 4.77 GHz **(b) At 6.23GHz**

Figure 2.17 Current density distribution at mode 4 (OFF-ON) (Dual band)

❖ Farfield Radiation Pattern

The simulated farfield radiation patterns of the antenna at the resonant frequencies of 4.77 GHz and 6.23 GHz in E-plane (φ=90°) and H-plane (φ= 0°) are illustrated in figures 2.18-21 respectively. In the E-plane, the pattern consists of mainly two lobes in upper and lower hemispheres respectively. However, in H-plane, we observe two lobes with significant contrast in beamwidths. Again, detailed radiation patterns information are indicated near the graphs.

At frequency 4.77 GHz

E-plane(φ=90°)

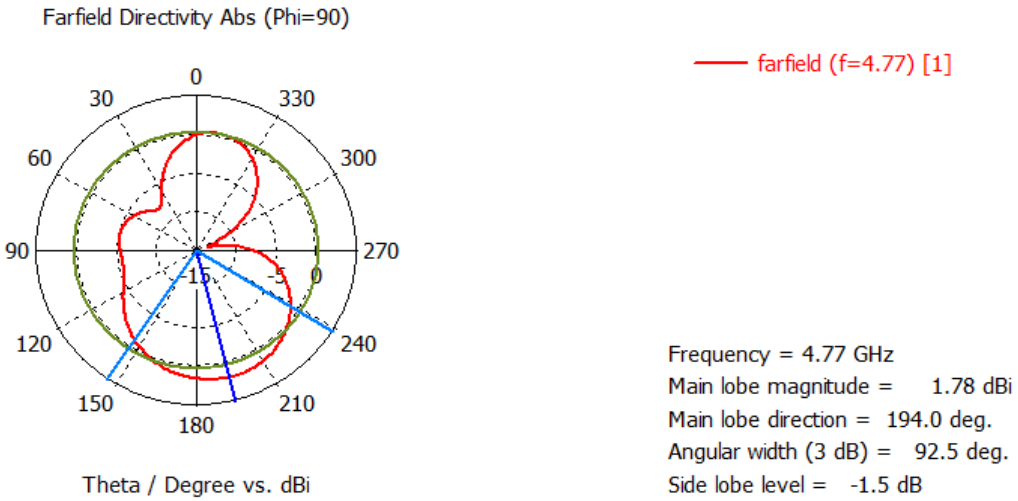

Figure 2.18 E-plane radiation pattern at 4.77 GHz

H-plane (φ= 0°)

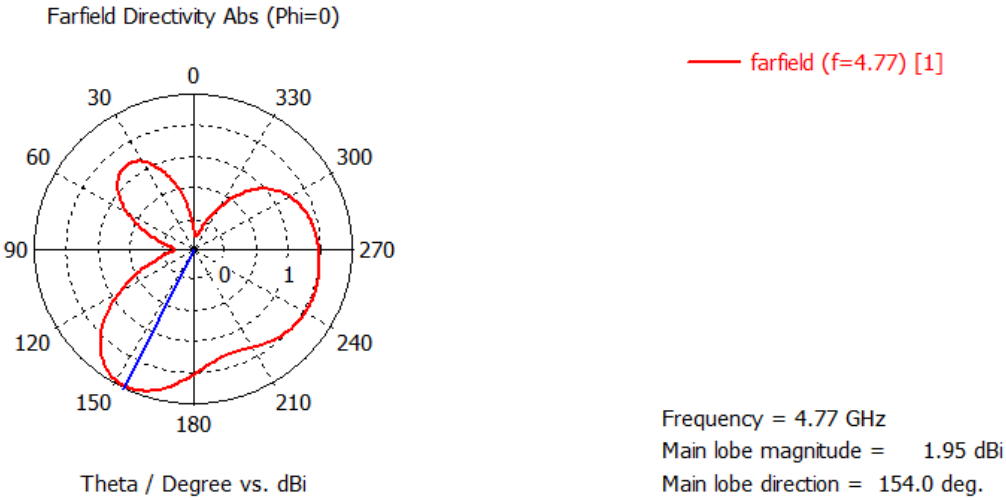

Figure 2.19 H-plane radiation pattern at 4.77 GHz

At frequency 6.23 GHz

E-plane(φ=90°)

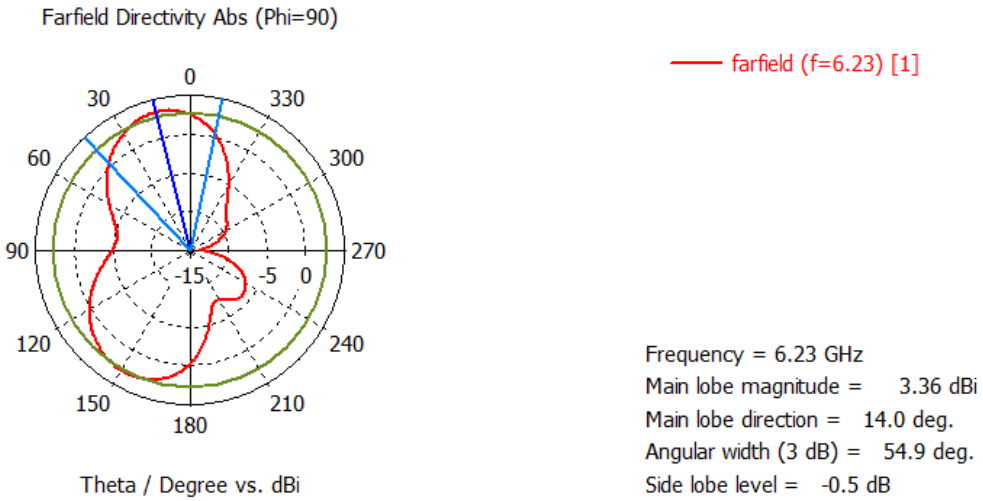

Figure 2.20 E-plane radiation pattern at 6.23 GHz

H-plane (φ= 0°)

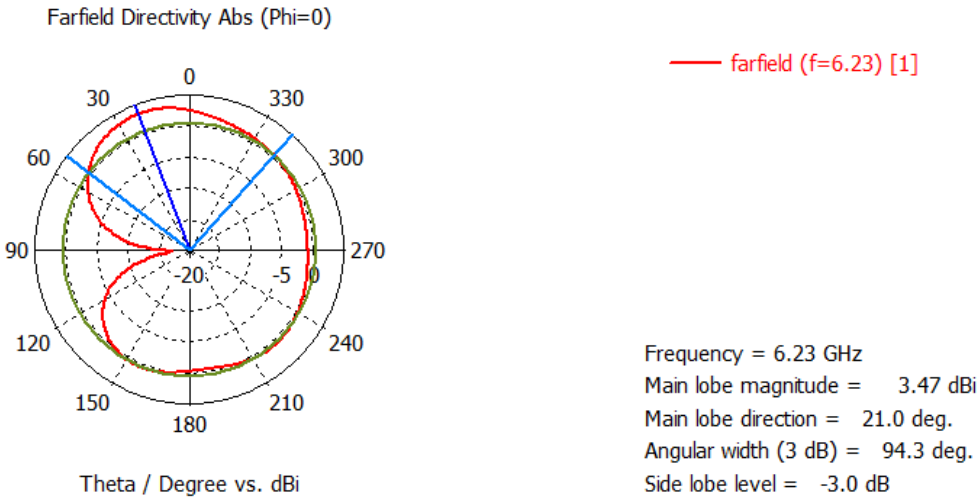

Figure 2.21 H-plane radiation pattern at 6.23 GHz

2.4 Antenna Characteristics

Table 2.3 summarizes the obtained monopole reconfigurable antenna radio electric characteristics at the different modes. Besides the observed behavior, it is seen from this table that the antenna shows significant efficiency of around 90% at different operating modes frequencies. Also, the antenna fits applications such as Wi-Fi- WiMAX, WLAN and in C-band.

Table 2.3 Summary of results

Parameters	Mode 1	Mode 2		Mode 3	Mode 4	
Nature	Single-band	Dual-band		Single-band	Dual-band	
Frequencies(GHz)	5.18	2.44	6.27	3.77	4.77	6.23
Bandwidth (MHz)	1745	533	1080	1441	1416	1582
Gain(dBi)	1.99	2.08	3.88	2.7	1.82	3.79
Directivity(dBi)	2.51	2.45	4.52	3.44	2.37	4.49
Efficiency (%)	88.7	91.7	86.3	84.4	88.1	85.24

2.5 Fabrication and Measurement

The modified E-shape antenna is fabricated and tested. Figure 2.22 shows the photograph of the fabricated antenna. The measured and simulated reflection coefficients in the first mode are shown in Figure 2.23**.** It can be observed that the simulated and measured results are in good agreement. The observed shift may be attributed to the difference between simulated and practical geometrical and physical parameters, the fabrication process as well as to the experimental conditions.

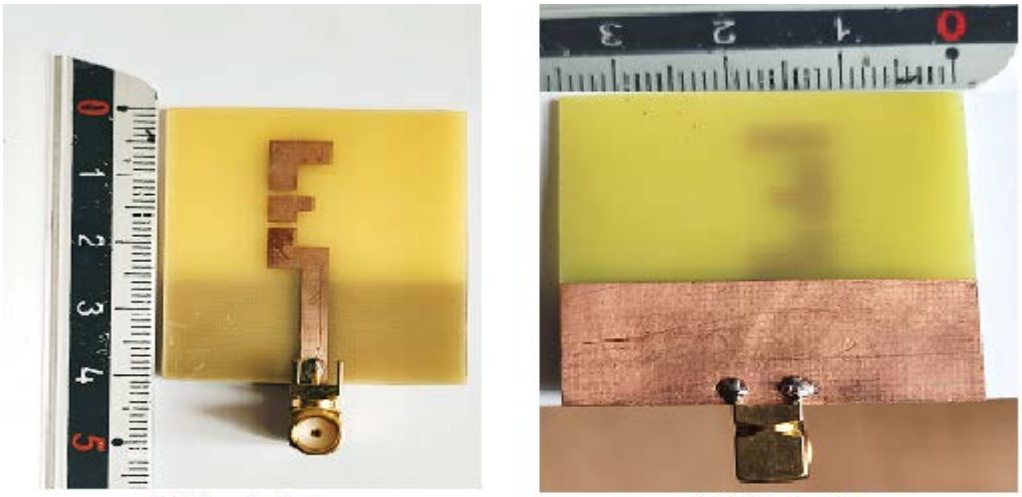

(a) Front view (b) Back view

Figure 2.22 Photograph of the fabricated modified E-shape antenna prototype

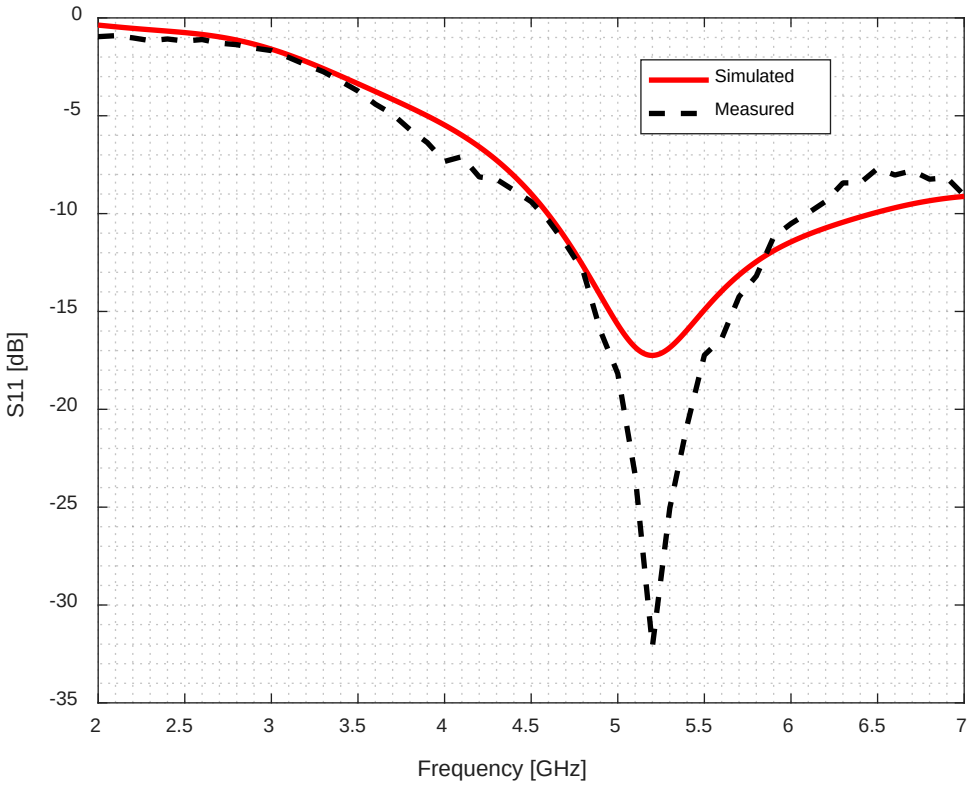

Figure 2.23 Simulated and measured reflection coefficients of modified antenna

2.6 Conclusion

Using the two switches (s1, s2), a reconfigurable an E-shaped multi-band monopole antenna using the available substrate material has been obtained. The antenna operates in two-dual band and two single-band modes, depending on the state of the switches.

The antenna has been fabricated and its reflection coefficient at the first mode is measured where a good agreement is observed with the simulated results.

Starting from this configuration, modifications will be performed in the next chapter to develop and investigate different configurations.

Chapter Three

Parametric Analysis of Reconfigurable Multi-Band Antenna

3.1 Introduction

In the previous chapter, analysis of a reconfigurable E-shape antenna has been performed, where the antenna operates in two dual-band and two single-band modes depending on the states of the two switches (s1, s2).

A parametric study is performed in this chapter where the main objective is to get and describe the antenna behavior at different slots positions. In order to reach these objectives, we changed the two slots' positions, as a result different structures have been obtained.

In the final part, we suggest a structure for further analysis and fabrication.

3.2 Simulation results of different structures

Figure 3.1 shows the assumed slots positions taken for the parametric study of the antenna, for each switch (s1, s2) three positions have been considered:

- **Position 0 :** Slot at the bottom of the corresponding vertical segment of the E-shape ;
- **Position 1 :** Slot in the middle of the corresponding vertical segment of the E-shape ;
- **Position 2:** Slot at the top side of the corresponding vertical segment, before the horizontal segment of the E-shape

It is also important to mention that this partitioning is motivated by the comparable size of the vertical segments with respect to the slots thickness (around three times). Also, intermediate slots positions didn't show significant change in the antenna band characteristics behavior.

Consequently, the simulations ended-up with nine main configurations that are reported in the following sections.

Also, in what fellows the structures (configurations) are numbered as indicated in this table:

Table 3.1 Structure number and slots positions

Structure N°	1	2	3	4	5	6	7	8	9
Slot 1 position	0	1	2	0	1	2	0	1	2
Slot 2 position	0	0	0	1	1	1	2	2	2

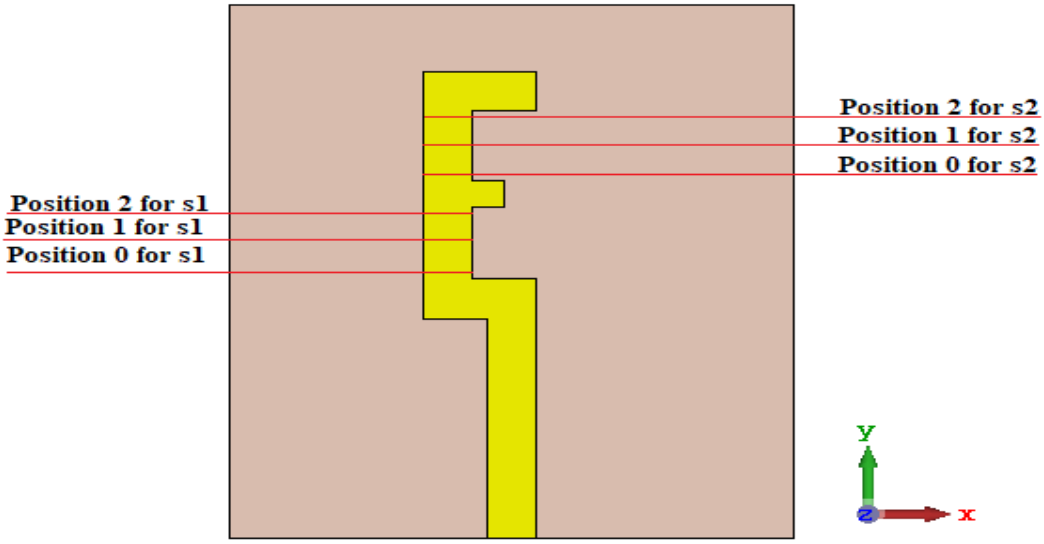

Figure 3.1 Slots positions

- **Structure 1 (s1 in position 0 & s2 is in position 0)**

Figure 3.2 shows the layout of structure 1. Slot 1, and slot 2 are in position 0.

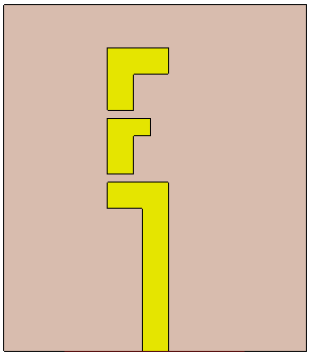

Figure 3.2 Layout of structure 1

❖ Reflection coefficient

When both switches (s1, s2) are turned OFF the antenna operates in mode 1. In this mode, the antenna acts as a single-band antenna (5.69 GHz) having a minimum simulated reflection coefficient of -29 dB and a bandwidth of 4.16 GHz (5 – 9.16 GHz). If both switches are turned ON, the antenna operates in mode 2. In this mode, it acts as a dual-band antenna (2.44 GHz and 6.29 GHz) having minimum simulated reflection coefficients of -24.22 dB and -34.64 dB and bandwidths of 0.53 GHz (2.22 – 2.75 GHz) and 1.11 GHz (5.88 – 6.99 GHz) for frequencies of 2.44 GHz and 6.29 GHz respectively. When switch s1 is ON and switch s2 is OFF the antenna operates in single mode 3 (3.81 GHz), with a minimum simulated reflection coefficient of -27.58 dB and bandwidth of 1.5 GHz (3.08 – 4.58 GHz). When switch s1 is OFF and switch s2 is ON, the proposed antenna operates

in mode 4 as a single-band (6.54 GHz), with a minimum simulated reflection coefficient of -32.52 dB and bandwidth of 2.96 GHz (5.94 – 8.90 GHz). Figure 3.2 shows the reflection coefficients of the four modes.

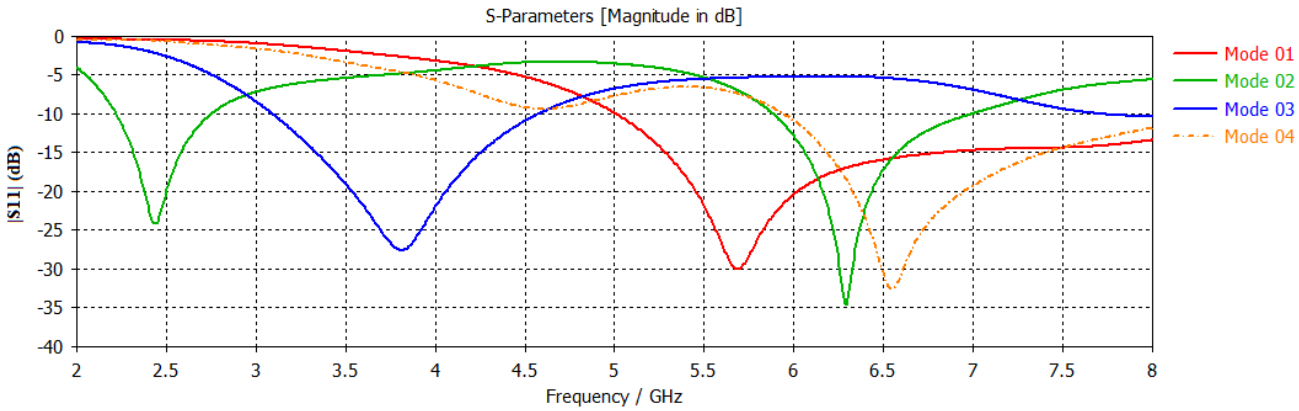

Figure 3.3 Reflection Coefficients of structure 1

- **Structure 2 (s1 in position 1 & s2 is in position 0)**

Figure 3.4 shows the layout of structure 2. Slot 1 is in position 1 and slot 2 is in position 0.

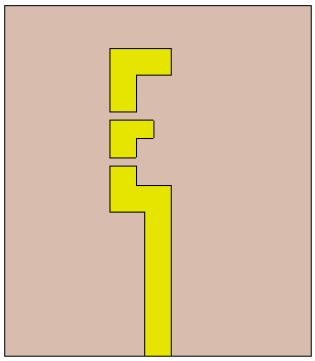

Figure 3.4 Layout of structure 2

❖ Reflection coefficients

When both the switches (s1, s2) are turned OFF the antenna operates in mode 1, in this mode, the antenna acts as a single-band antenna (5.38 GHz) having a minimum simulated reflection coefficient of -19.44 dB and bandwidth of 2.45 GHz (4.75 – 7.2 GHz). If both switches are turned ON, the antenna operates in mode 2. In this mode, it acts as a dual-band antenna (2.44 GHz and 6.29 GHz) having minimum simulated reflection coefficients of -24.22 dB and -34.64 dB and bandwidths of 0.53 GHz (2.22 – 2.75 GHz) and 1.11 GHz (5.88 – 6.99 GHz) for frequencies of 2.44 GHz and 6.29 GHz respectively. When switch s1 is ON and switch s2 is OFF the antenna works in single mode 3

(3.81 GHz), with a minimum simulated reflection coefficient of -27.58 dB and bandwidth of 1.5 GHz (3.08 – 4.58 GHz). When switch s1 is OFF and switch s2 is ON, the proposed antenna operates in mode 4 as a dual-band (4.81 GHz and 6.25 GHz), with minimum simulated reflection coefficients of -18.32dB and -30.11dB, and bandwidths of 1.24 GHz (4.30 – 5.54 GHz) and 1.87 GHz (5.54 – 7.41 GHz) for frequencies of 4.81 GHz and 6.25 GHz respectively. Figure 3.5 shows the reflection coefficients of the four modes.

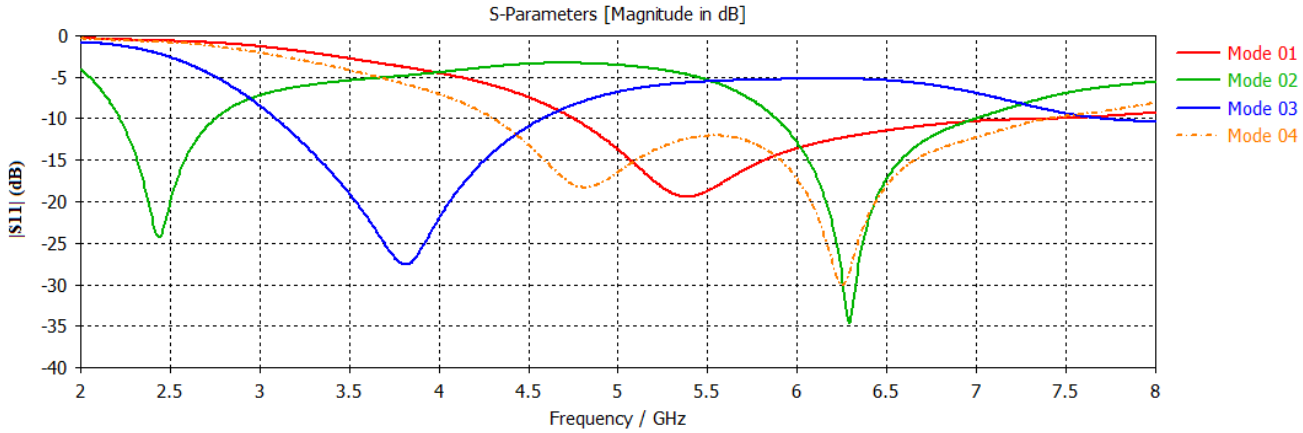

Figure 3.5 Reflection Coefficients of structure 2

- **Structure 3 (s1 in position 2 & s2 is in position 0)**

Figure 3.6 shows the layout of structure 3. Slot 1 is in position 2 and slot 2 is in position 0.

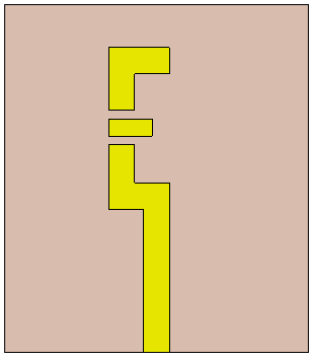

Figure 3.6 Layout of structure 3

❖ Reflection coefficients

When both the switches (s1, s2) are turned OFF the antenna operates in mode 1, in this mode, the antenna acts as a single-band antenna (4.84 GHz) having a minimum simulated reflection coefficient of -16.57dB and bandwidth of 1.38 GHz (4.25 – 5.63 GHz). If both switches are turned ON, the

antenna operates in mode 2. In this mode, it acts as a dual-band antenna (2.44 GHz and 6.29 GHz) having minimum simulated reflection coefficients of -24.22 dB and -34.64 dB and bandwidths of 0.53 GHz (2.22 – 2.75 GHz) and 1.11 GHz (5.88 – 6.99 GHz) for frequencies of 2.44 GHz and 6.29 GHz respectively. When switch s1 is ON and switch s2 is OFF the antenna works in single mode 3 (3.81 GHz), with a minimum simulated reflection coefficient of -27.58 dB and bandwidth of 1.5 GHz (3.08 – 4.58 GHz). When switch s1 is OFF and switch s2 is ON, the proposed antenna operates in mode 4 as a dual-band (4.57 GHz and 6.36 GHz), with minimum simulated reflection coefficients of -41.65dB and -17.98dB, and bandwidths of 1.73 GHz (3.87 – 5.6 GHz) and 1.34 GHz (5.6 – 6.94 GHz) for frequencies of 4.57 GHz and 6.36 GHz respectively. Figure 3.7 shows the reflection coefficients of the four modes.

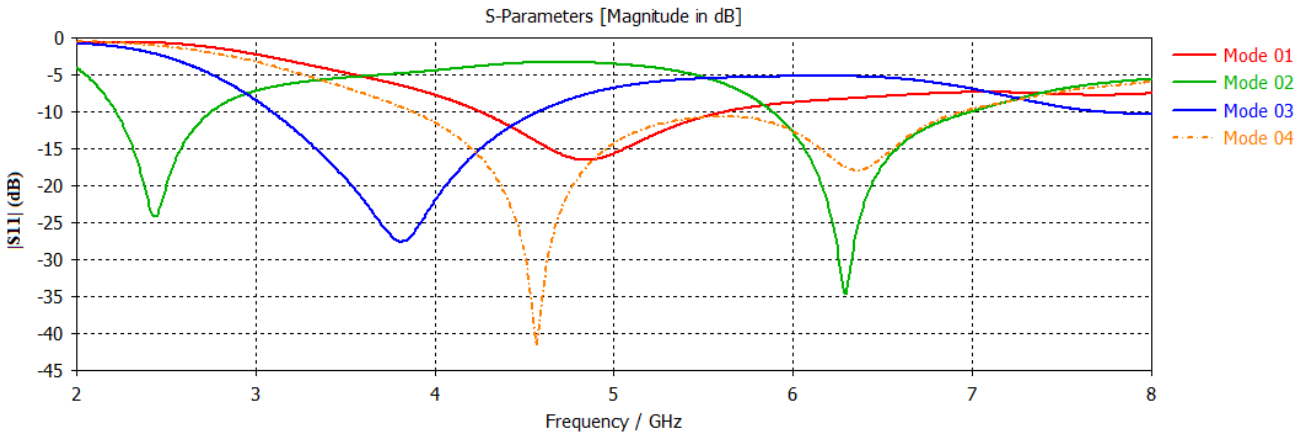

Figure 3.7 Reflection Coefficients of structure 3

- **Structure 4 (s1 in position 0 & s2 is in position 1)**

Figure 3.8 shows the layout of structure 4. Slot 1 is in position 2 and slot 2 is in position 1.

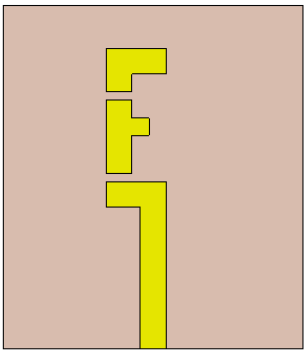

Figure 3.8 Layout of structure 4

❖ Reflection coefficients

When both the switches (s1, s2) are turned OFF the antenna operates in mode 1, in this mode, the antenna acts as a single-band antenna (5.59 GHz) having a minimum simulated reflection coefficient of -28.73dB and bandwidth of 4.52 GHz (4.94 – 9.46 GHz). If both switches are turned ON, the antenna operates in mode 2. In this mode, it acts as a dual-band antenna (2.44 GHz and 6.29 GHz) having minimum simulated reflection coefficients of -24.22 dB and -34.64 dB and bandwidths of 0.53 GHz (2.22 – 2.75 GHz) and 1.11 GHz (5.88 – 6.99 GHz) for frequencies of 2.44 GHz and 6.29 GHz respectively. When switch s1 is ON and switch s2 is OFF the antenna works in single mode 3 (3.4 GHz), with a minimum simulated reflection coefficient of -25.28 dB and bandwidth of 1.45 GHz (2.9 – 4.35 GHz). When switch s1 is OFF and switch s2 is ON, the proposed antenna operates in mode 4 as a single-band (6.54 GHz), with a minimum simulated reflection coefficient of -32.52dB and bandwidth of 2.96 GHz (5.94 – 8.90 GHz). Figure 3.9 shows the reflection coefficients of the four modes.

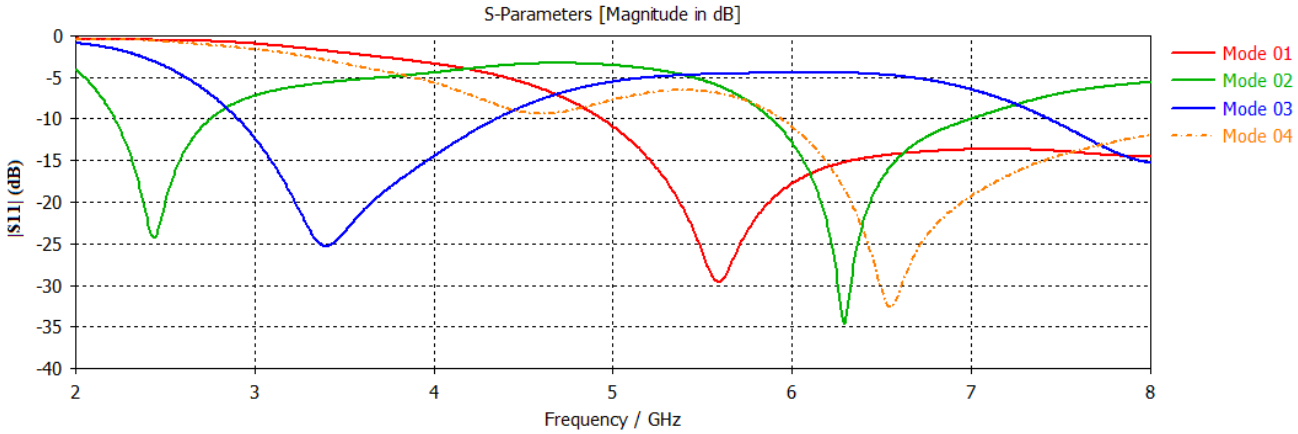

Figure 3.9 Reflection Coefficients of structure 4

- ## Structure 5 (s1 in position 1 & s2 is in position 1)

Figure 3.10 shows the layout of structure 5. Slot 1 is in position 1 and slot 2 is in position 1.

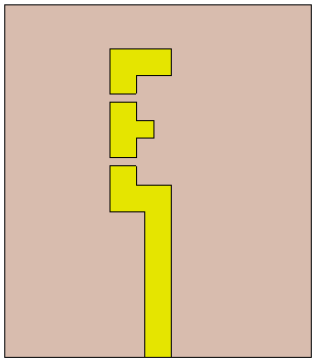

Figure 3.10 Layout of structure 5

❖ Reflection coefficients

When both the switches (s1, s2) are turned OFF the antenna operates in mode 1, in this mode, the antenna acts as a single-band antenna (5.33 GHz) having a minimum simulated reflection coefficient of -19.25 dB and bandwidth of 2.2 GHz (4.7 – 6.9 GHz). If both switches are turned ON, the antenna operates in mode 2. In this mode, it acts as a dual-band antenna (2.44 GHz and 6.29 GHz) having minimum simulated reflection coefficients of -24.22 dB and -34.64 dB and bandwidths of 0.53 GHz (2.22 – 2.75 GHz) and 1.11 GHz (5.88 – 6.99 GHz) for frequencies of 2.44 GHz and 6.29 GHz respectively. When switch s1 is ON and switch s2 is OFF the antenna works in single mode 3 (3.4 GHz), with simulated reflection coefficient of -25.28 dB and bandwidth of 1.45 GHz (2.9 – 4.35 GHz). When switch s1 is OFF and switch s2 is ON, the proposed antenna operates in mode 4 as a dual-band (4.81 GHz and 6.25 GHz), with minimum simulated reflection coefficients of -18.32dB and -30.11dB and bandwidths of 1.24 GHz (4.30 – 5.54 GHz) and 1.87 GHz (5.54 – 7.41 GHz) for frequencies of 4.81 GHz and 6.25 GHz respectively. Figure 3.11 shows the reflection coefficients of the four modes.

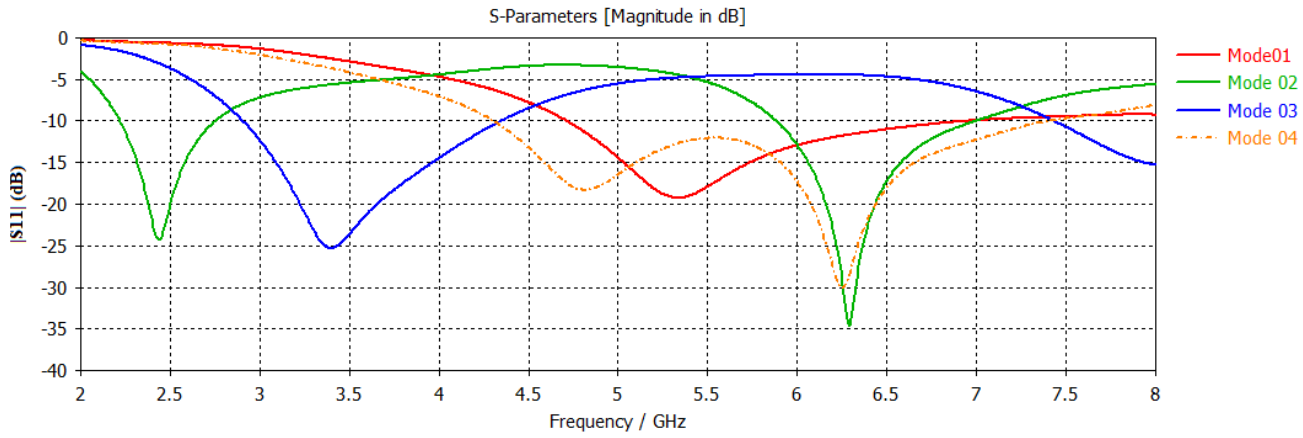

Figure 3.11 Reflection Coefficients of structure 5

- **Structure 6 (s1 in position 2 & s2 is in position 1)**

Figure 3.12 shows the layout of structure 6. Slot 1 is in position 2 and slot 2 is in position 1.

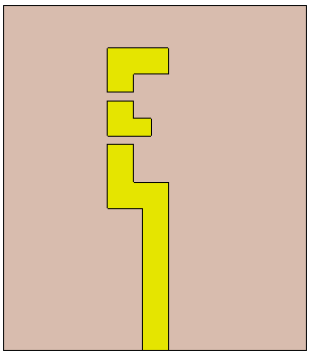

Figure 3.12 Layout of structure 6

❖ Reflection coefficients

When both the switches (s1, s2) are turned OFF the antenna operates in mode 1, in this mode, the antenna acts as a single-band antenna (4.81 GHz) having a minimum simulated reflection coefficient of -16.3dB and bandwidth of 1.32 GHz (4.23 – 5.55 GHz). If both switches are turned ON, the antenna operates in mode 2. In this mode, it acts as a dual-band antenna (2.44 GHz and 6.29 GHz) having minimum simulated reflection coefficients of -24.22 dB and -34.64 dB and bandwidths of 0.53 GHz (2.22 – 2.75 GHz) and 1.11 GHz (5.88 – 6.99 GHz) for frequencies of 2.44 GHz and 6.29 GHz respectively. When switch s1 is ON and switch s2 is OFF the antenna works in single mode 3 (3.4 GHz), with a minimum simulated reflection coefficient of -25.28 dB and bandwidth of 1.45 GHz (2.9 – 4.35 GHz). When switch s1 is OFF and switch s2 is ON, the proposed antenna operates in mode 4 as a dual-band (4.57 GHz and 6.36 GHz), with minimum simulated reflection coefficients of -41.65dB and -17.98dB and bandwidths of 1.73 GHz (3.87 – 5.6 GHz) and 1.34 GHz (5.6 – 6.94

GHz) for frequencies of 4.57 GHz and 6.36 GHz respectively. Figure 3.13 shows the reflection coefficients of the four modes.

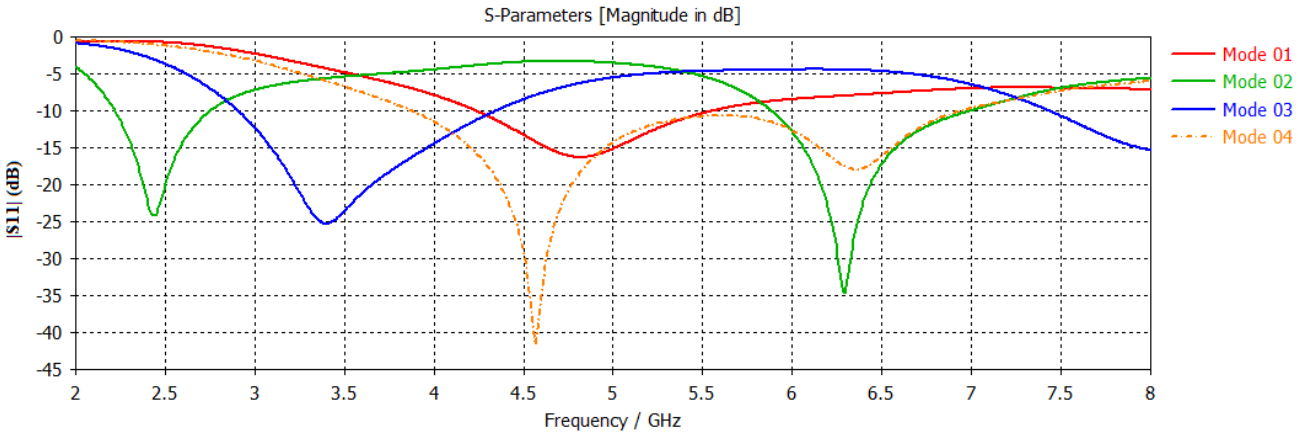

Figure 3.13 Reflection Coefficients of structure 6

- **Structure 7 (s1 in position 0 & s2 is in position 2)**

Figure 3.14 shows the layout of structure 7. Slot 1 is in position 0 and slot 2 is in position 2.

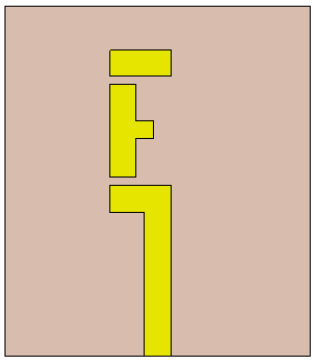

Figure 3.14 Layout of structure 7

❖ **Reflection coefficients**

When both the switches (s1, s2) are turned OFF the antenna operates in mode 1, in this mode, the antenna acts as a dual-band antenna (5.42 GHz and 7.6 GHz) having minimum simulated reflection coefficients of -22.88 dB and -18.87 dB and bandwidths of 1.71 GHz (4.83 – 6.54 GHz) and 2.94 GHz (6.54 – 9.48 GHz) for frequencies of 5.42 GHz and 7.6 GHz respectively. If both switches are turned ON, the antenna operates in mode 2. In this mode, it acts as a dual-band antenna (2.44 GHz and 6.29 GHz) having minimum simulated reflection coefficients of -24.22 dB and -34.64 dB and bandwidths of 0.53 GHz (2.22 – 2.75 GHz) and 1.11 GHz (5.88 – 6.99 GHz) for frequencies of 2.44 GHz and 6.29 GHz respectively. When switch s1 is ON and switch s2 is OFF the antenna works in

dual-band mode 3 (3.08 GHz and 7.66 GHz), with simulated reflection coefficients of -30.47 dB and -19.63 dB and bandwidths of 1.25 GHz (2.7 – 3.95 GHz) and 2 GHz (7 – 9GHz) for frequencies of 3.08 GHz and 7.66 GHz respectively. When switch s1 is OFF and switch s2 is ON, the proposed antenna operates in mode 4 as a single-band (6.54 GHz), with a minimum simulated reflection coefficient of -32.52dB and bandwidth of 2.96 GHz (5.94 – 8.90 GHz). Figure 3.15 shows the reflection coefficients of the four modes.

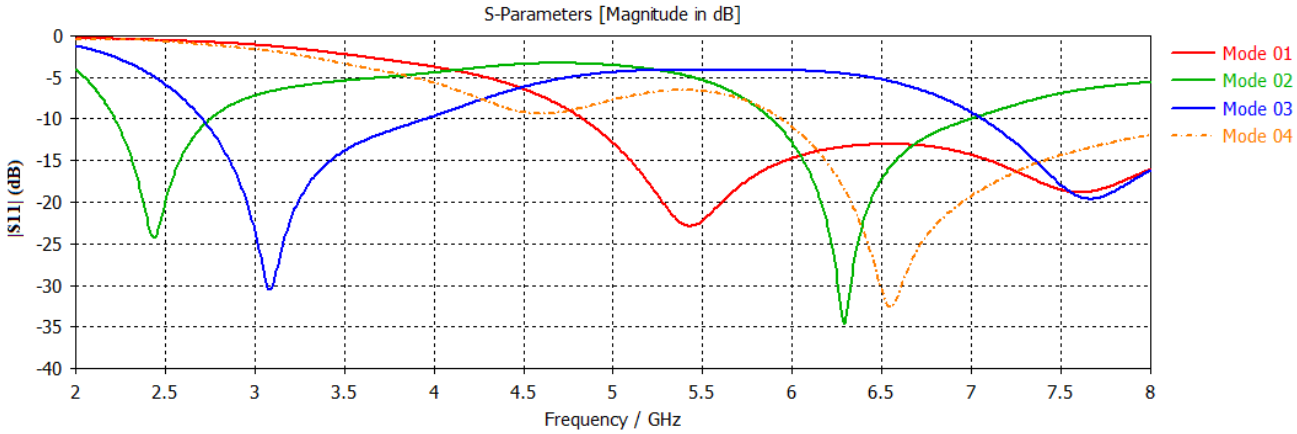

Figure 3.15 Reflection Coefficients of structure 7

Structure 8 (s1 in position 1 & s2 is in position 2)

Figure 3.16 shows the layout of structure 8. Slot 1 is in position 1 and slot 2 is in position 2.

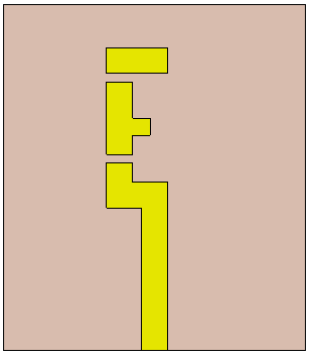

Figure 3.16 Layout of structure 8

❖ Reflection coefficients

When both the switches (s1, s2) are turned OFF the antenna operates in mode 1, in this mode, the antenna acts as a single-band antenna (5.25 GHz) having a minimum simulated reflection coefficient of -21.37dB and bandwidth of 2.37 GHz (4.63 – 7GHz). If both switches are turned ON, the antenna operates in mode 2. In this mode, it acts as a dual-band antenna (2.44 GHz and 6.29 GHz) having minimum simulated reflection coefficients of -24.22 dB and -34.64 dB and bandwidths of 0.53 GHz

(2.22 – 2.75 GHz) and 1.11 GHz (5.88 – 6.99 GHz) for frequencies of 2.44 GHz and 6.29 GHz respectively. When switch s1 is ON and switch s2 is OFF the antenna works in dual-band mode 3 (3.08 GHz and 7.66 GHz), with minimum simulated reflection coefficients of -30.47 dB and -19.63 dB and bandwidths of 1.25 GHz (2.7 – 3.95 GHz) and 2 GHz (7 – 9GHz) for frequencies of 3.08 GHz and 7.66 GHz respectively. When switch s1 is OFF and switch s2 is ON, the proposed antenna operates in mode 4 as a dual-band (4.81 GHz and 6.25 GHz), with minimum simulated reflection coefficients of -18.32dB and -30.11dB, and bandwidths of 1.24 GHz (4.30 – 5.54 GHz) and 1.87 GHz (5.54 – 7.41 GHz) for frequencies of 4.81 GHz and 6.25 GHz respectively. Figure 3.17 shows the reflection coefficients of the four modes.

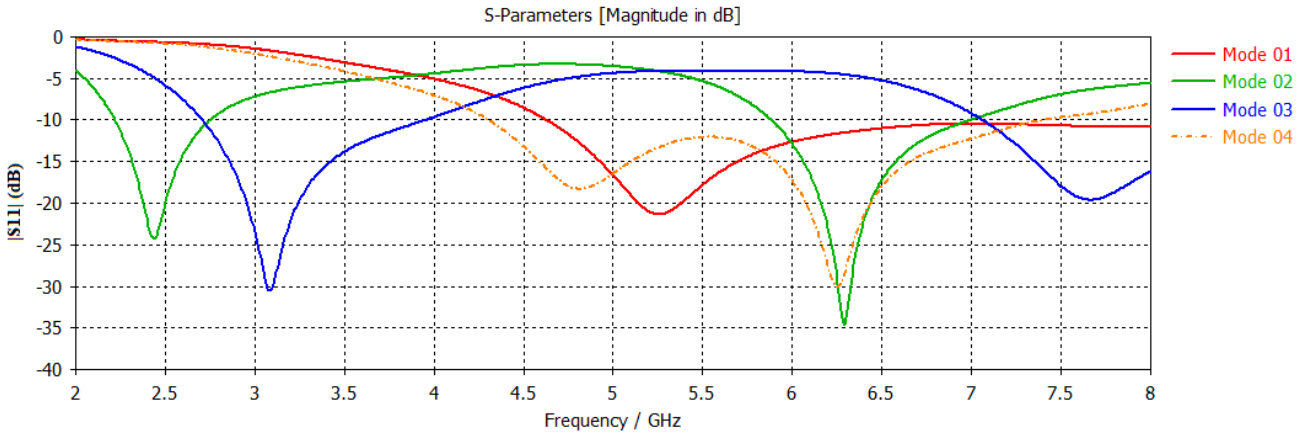

Figure 3.17 Reflection Coefficients of structure 8

- **Structure 9 (s1 in position 2 & s2 is in position 2)**

Figure 3.18 shows the layout of structure 08. Slot 1 is in position 2 and slot 2 is in position 2.

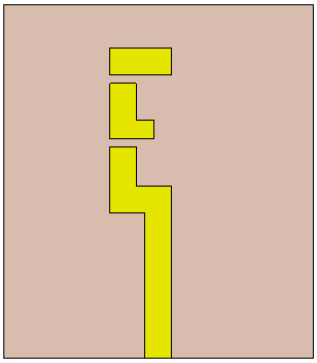

Figure 3.18 Layout of structure 09

❖ Reflection coefficients

When both the switches (s1, s2) are turned OFF the antenna operates in mode 1, in this mode, the antenna acts as a single-band antenna (4.77 GHz) having a minimum simulated reflection coefficient of -17.26dB and bandwidth of 1.33 GHz (4.2 – 5.53 GHz). If both switches are turned ON, the antenna operates in mode 2. In this mode, it acts as a dual-band antenna (2.44 GHz and 6.29 GHz) having minimum simulated reflection coefficients of -24.22 dB and -34.64 dB and bandwidths of 0.53 GHz (2.22 – 2.75 GHz) and 1.11 GHz (5.88 – 6.99 GHz) for frequencies of 2.44 GHz and 6.29 GHz respectively. When switch s1 is ON and switch s2 is OFF the antenna works in dual-band mode 03 (3.08 GHz and 7.66 GHz) with simulated reflection coefficients of -30.47 dB and -19.63 dB and bandwidths of 1.25 GHz (2.7 – 3.95 GHz) and 2 GHz (7 – 9GHz) for frequencies of 3.08 GHz and 7.66 GHz respectively. When switch s1 is OFF and switch s2 is ON, the proposed antenna operates in mode 4 as a dual-band (4.57 GHz and 6.36 GHz), with minimum simulated reflection coefficients of -41.65dB and -17.98dB and bandwidths of 1.73 GHz (3.87 – 5.6 GHz) and 1.34 GHz (5.6 – 6.94 GHz) for frequencies of 4.57 GHz and 6.36 GHz respectively. Figure 3.19 shows the reflection coefficients of the four modes.

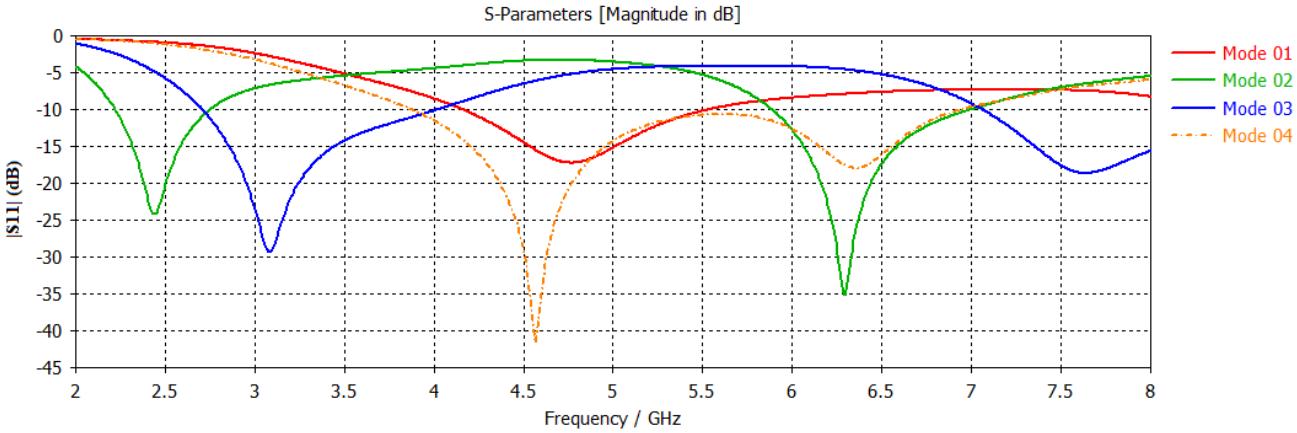

Figure 3.19 Reflection Coefficients of structure 9

Finally, Table 3.1 shows the summarized band characteristics (operating frequencies) of the investigated reconfigurable antennas configurations at the different modes and where it is observed that these structures fit several applications.

Table 3.2 Summary of resulted modes frequencies

Antenna configuration (Structure)	Slots positions		Frequency at each mode in GHz			
	s1	s2	Mode 1 OFF-OFF	Mode 2 ON-ON	Mode 3 ON-OFF	Mode 4 OFF-ON
Configuration 1	**0**	**0**	**5.69**	**2.44 & 6.29**	**3.81**	**6.54**
Configuration 2	**1**	**0**	**5.38**	**2.44 & 6.29**	**3.81**	**4.81 & 6.25**
Configuration 3	**2**	**0**	**4.84**	**2.44 & 6.29**	**3.81**	**4.57 & 6.36**
Configuration 4	**0**	**1**	**5.59**	**2.44 & 6.29**	**3.4**	**6.54**
Configuration 5	**1**	**1**	**5.33**	**2.44 & 6.29**	**3.4**	**4.81 & 6.25**
Configuration 6	**2**	**1**	**4.81**	**2.44 & 6.29**	**3.4**	**4.57 & 6.36**
Configuration 7	**0**	**2**	**5.42 & 7.6**	**2.44 & 6.29**	**3.08 & 7.66**	**6.54**
Configuration 8	**1**	**2**	**5.25**	**2.44 & 6.29**	**3.08 & 7.66**	**4.81 & 6.25**
Configuration 9	**2**	**2**	**4.77**	**2.44 & 6.29**	**3.08 & 7.66**	**4.57 & 6.36**

3.3 Further analysis of structure 8

For further study and manufacture, we picked structure 8 as a suggestion since it exhibits one single-band and three dual-bands operating modes. Also, this antenna is suitable for various applications including Wi-Fi, WLAN and Radar.

The switching states and the resulting operating frequencies are summarized in Table 3.2.

Table 3.3 Switching states and reconfiguration of structure 8

Modes	**S1**	**S2**	**Frequency mode**
Mode 1	OFF	OFF	Single-band 5.25 GHz
Mode 2	ON	ON	Dual-band 2.44 GHz & 6.29GHz
Mode 3	ON	OFF	Dual-band 3.08 GHz & 7.66 GHz
Mode 4	OFF	ON	Dual-band 4.81 GHz & 6.25 GHz

Furthermore, the structure current density and radiation patterns at the different modes are described the following sections.

3.3.1 Mode 1 (OFF, OFF)

Current density distribution

Figure 3.20 shows the current density distribution at frequency 5.25 GHz. We observe that shows that the portion of the patch contributing in the generation of the resonant frequency lies along the feed line and under the first slot position.

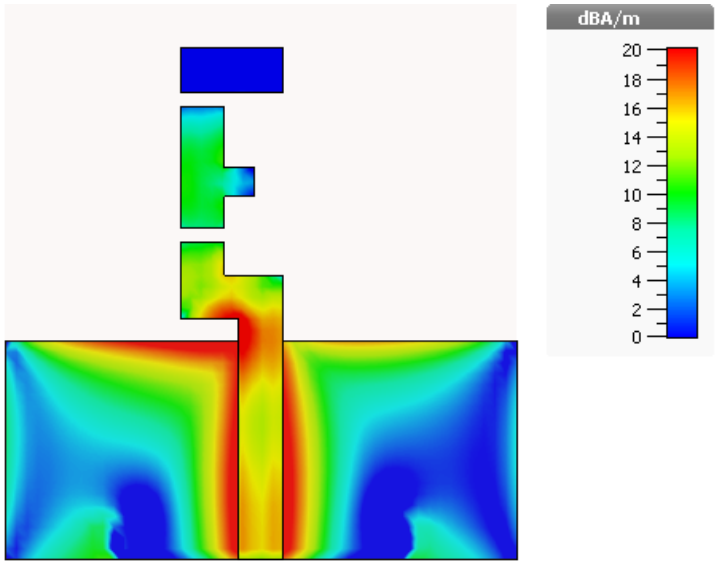

Figure 3.20 Current density distribution at mode 01 (OFF-OFF)
(single band = 5.25 GHz)

Farfield Radiation patterns

The simulated farfield radiation patterns of the antenna at resonance frequency of 5.25 GHz at E-plane (φ=90°) and H-plane (φ= 0°) are illustrated in figure 3.21 where we observe that the antenna presents a higher directivity in H-plane in the direction of around θ = 40°.

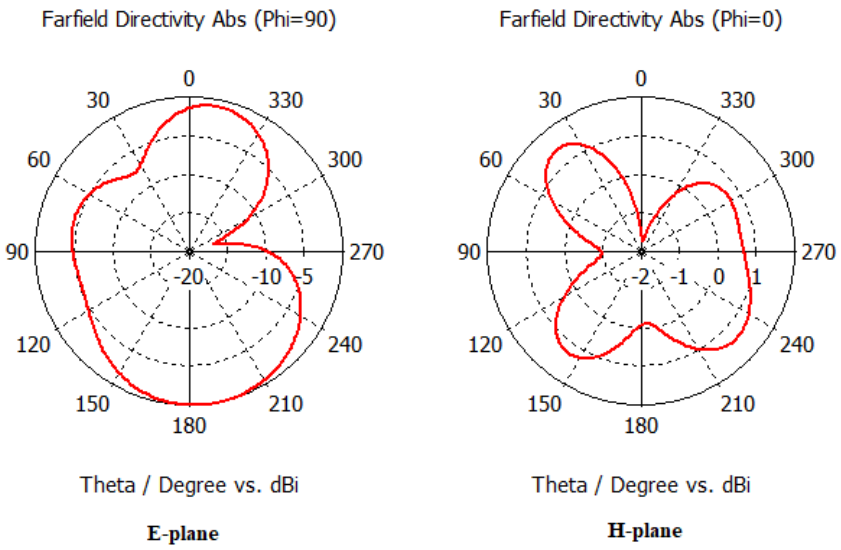

Figure 3.21 Radiation pattern at 5.25 GHz

3.3.2 Mode 2 (ON, ON)

Current density distribution

The current density distribution at the resonant frequencies of 2.44 and 6.29 GHz are illustrated in Figure 3.22. Figure 3.22 (a) shows the current density distribution at frequency 2.44 GHz where the surface current is maximum through the entire length of the radiating element and feed line.

Figure 3.22 (b) illustrates the current density distribution at frequency 6.29 GHz. The surface current density is higher along the feed line and the upper vertical segment of the E-shape structure.

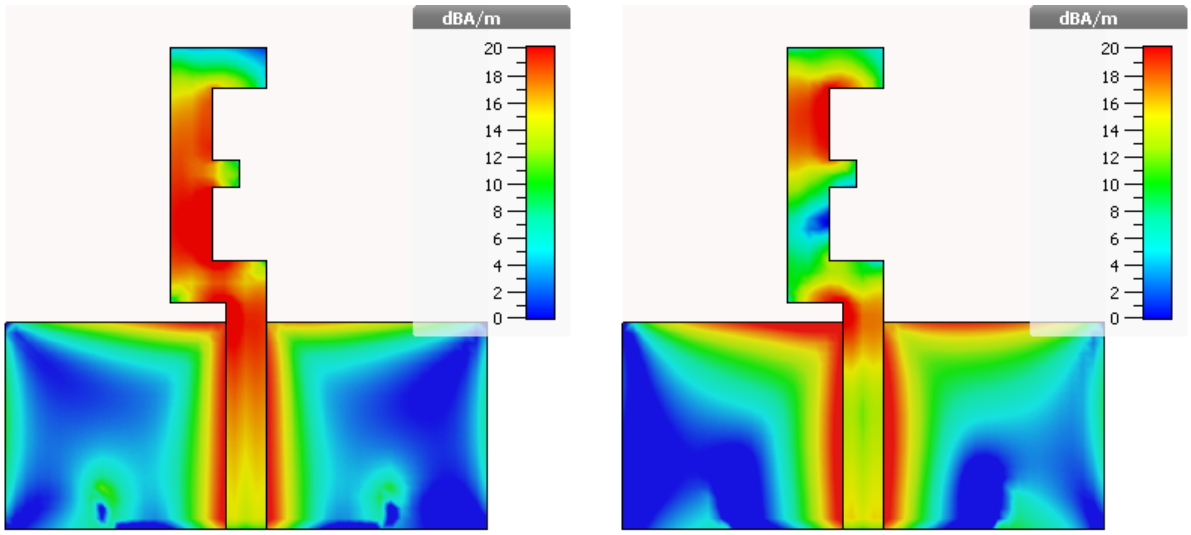

(a) At 2.44 GHz (b) At 6.29 GHz

Figure 3.22 Current density distribution at mode 02 (ON-ON) (Dual band)

Farfield Radiation patterns

The simulated farfield radiation patterns of the antenna at resonance frequencies of 2.44 GHz and 6.29 GHz E-plane (φ=90°) and H-plane (φ= 0°) are illustrated in figure 3.23 and figure 3.24 respectively. At the first resonance (2.44 GHz), the pattern is quasi omnidirectional whereas at the second (6.29 GHz), we observe two main lobes the two hemispheres.

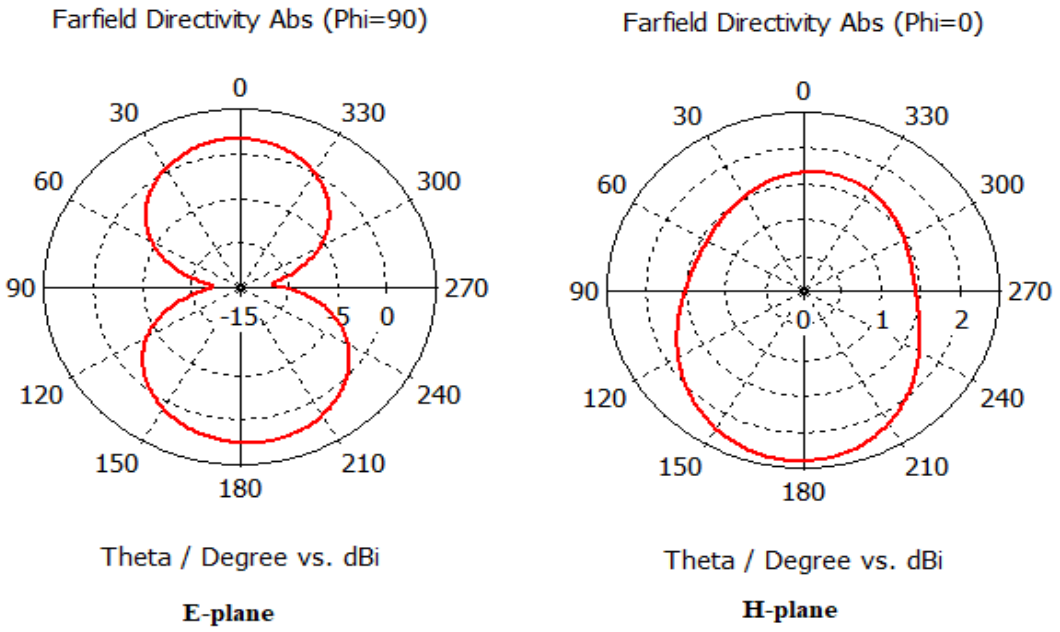

Figure 3.23 Radiation pattern at 2.44 GHz

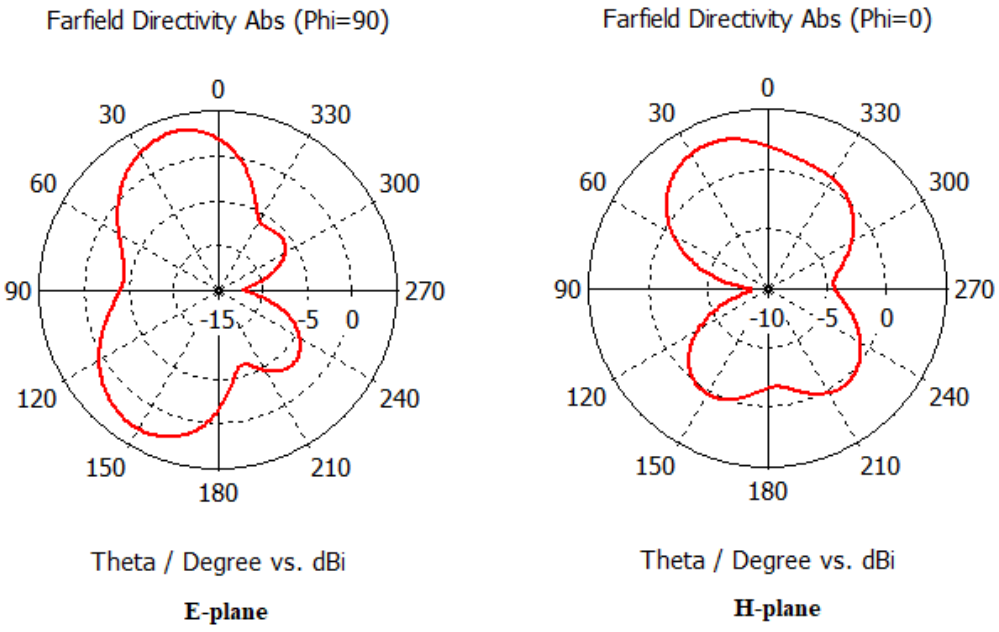

Figure 3.24 Radiation pattern at 6.29 GHz

3.3.3 Mode 3 (ON, OFF)

Current density distribution

The current density distribution at the resonant frequencies of 3.08 GHz and 7.66 GHz are illustrated in Figure 3.25. Figure 3.25 (a), shows the current density distribution at frequency 3.08 GHz, where the surface current is higher through the entire feed line and maximum along the lower segment of the E-shape structure. Figure 3.22. (b), illustrates the current density distribution at frequency 7.66 GHz. The surface current is concentrated along the feed line and has lower density in the upper vertical segment of the E-shape structure.

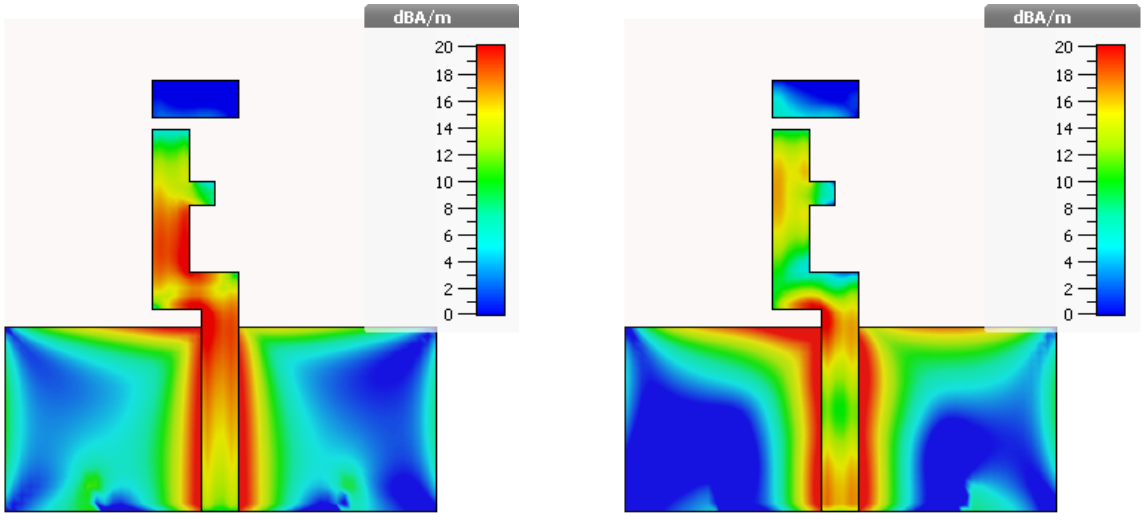

(a) At 3.08 GHz (b) At 7.66 GHz

Figure 3.25 Current density distribution at mode 03 (ON-OFF) (Dual band)

Farfield Radiation pattern

The simulated farfield radiation patterns of the antenna at resonance frequencies of 3.08 GHz and 7.66 GHz E-plane (φ=90°) and H-plane (φ= 0°) are illustrated in figure 3.26 and figure 3.27 respectively. Again, we notice an almost omnidirectional pattern at the first resonance whereas, at the second, the pattern is relatively directive in the direction θ = 25 ° in H-plane.

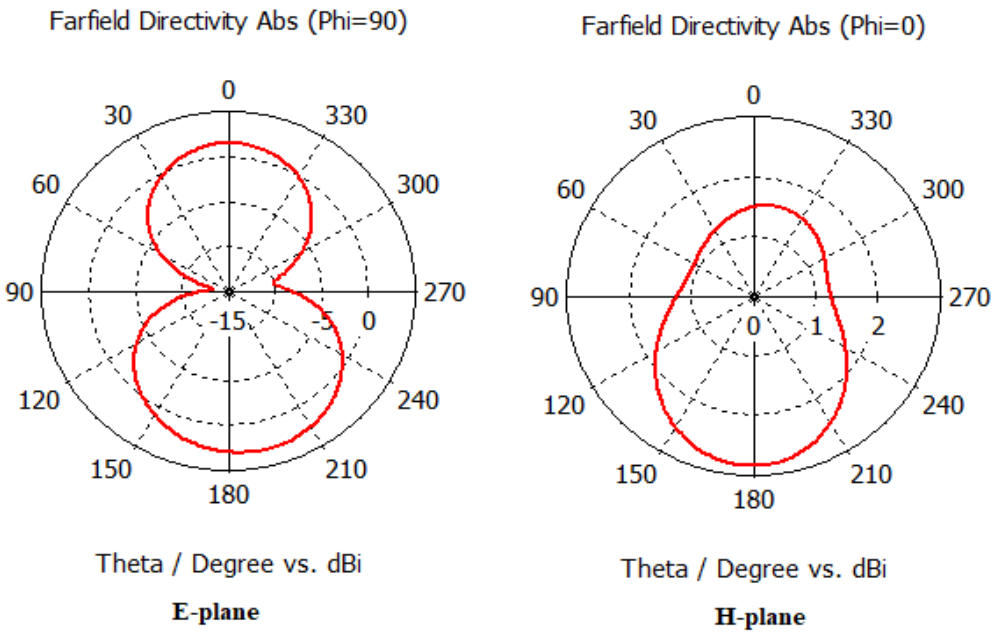

Figure 3.26 Radiation pattern at 3.08 GHz

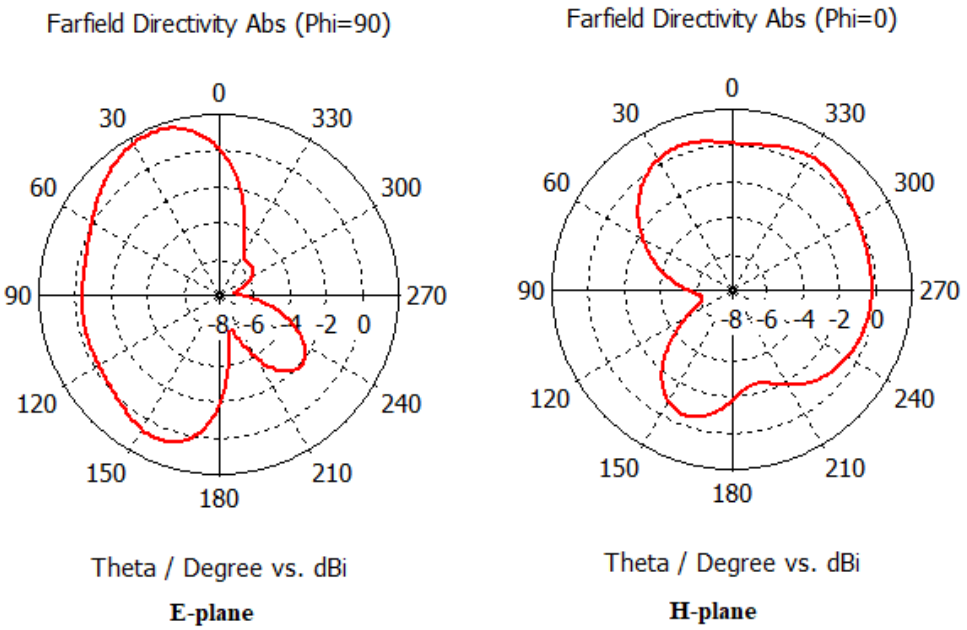

Figure 3.27 Radiation pattern at 7.66 GHz

3.3.4 Mode 4 (OFF, ON)

Current density distribution

The current density distribution at the resonant frequencies of 4.81 GHz and 6.25 GHz are shown in Figure 3.28. In figure 3.28 (a), the current density distribution at frequency 3.08 GHz is higher

through the entire feed line and upper segment of the E-shape structure. Figure 3.22. (b), illustrates the current density distribution at frequency 7.66 GHz. The surface current is concentrated along the feed line and has maximum density in the upper vertical segment of the E-shape structure.

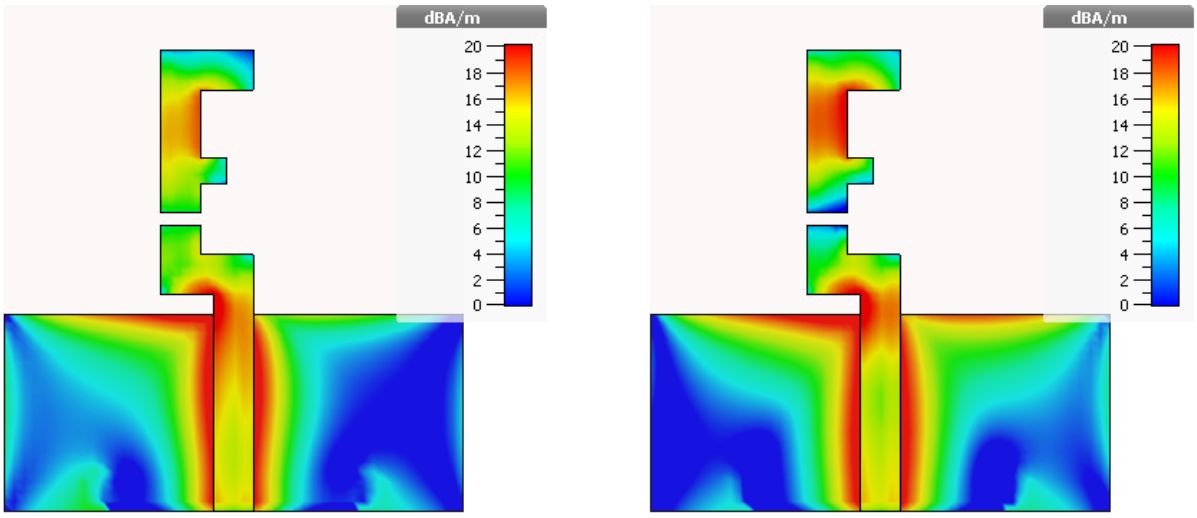

(a) At 4.81 GHz (b) At 6.25 GHz

Figure 3.28 Current density distribution at mode 04 (OFF-ON) (Dual band)

Farfield Radiation pattern

The simulated farfield radiation patterns of the antenna at resonance frequencies of 4.81 GHz and 6.25 GHz in E-plane (φ=90°) and H-plane (φ= 0°) are illustrated in figure 3.29 and figure 3.30 respectively. At the frequency 4.81 GHz, the pattern shows two main lobes in the E-plane whereas, in H-plane, we observe lobes with one having a large beamwidth. However, at the second resonance of 6.25 GHz, the pattern consists of two main lobes in both principle planes direct in the two hemispheres.

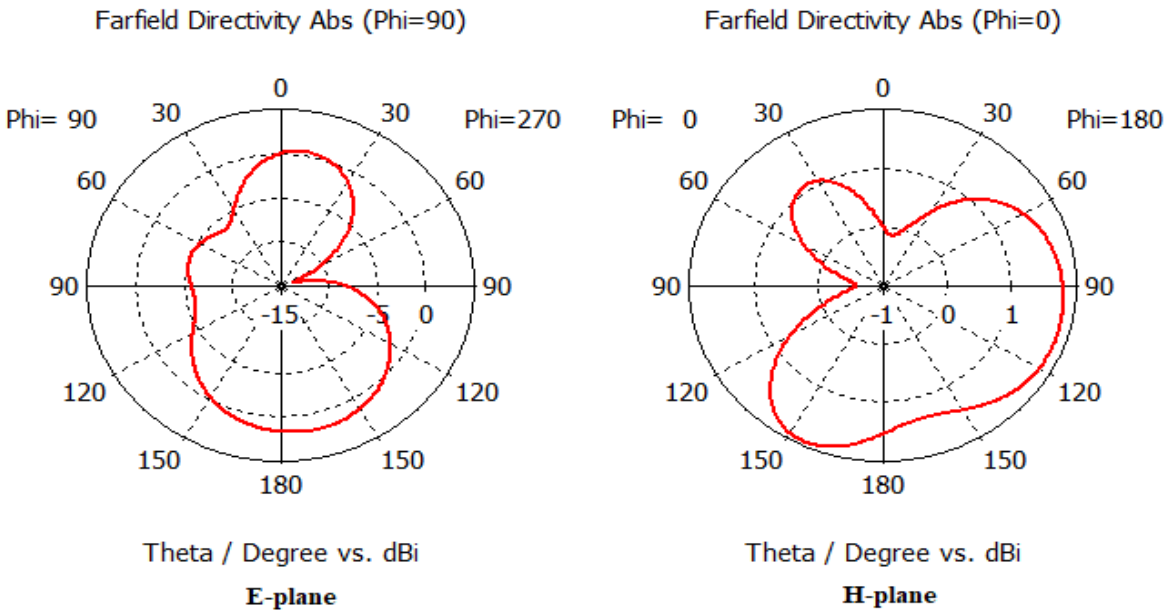

Figure 3.29 Radiation pattern at 4.81 GHz

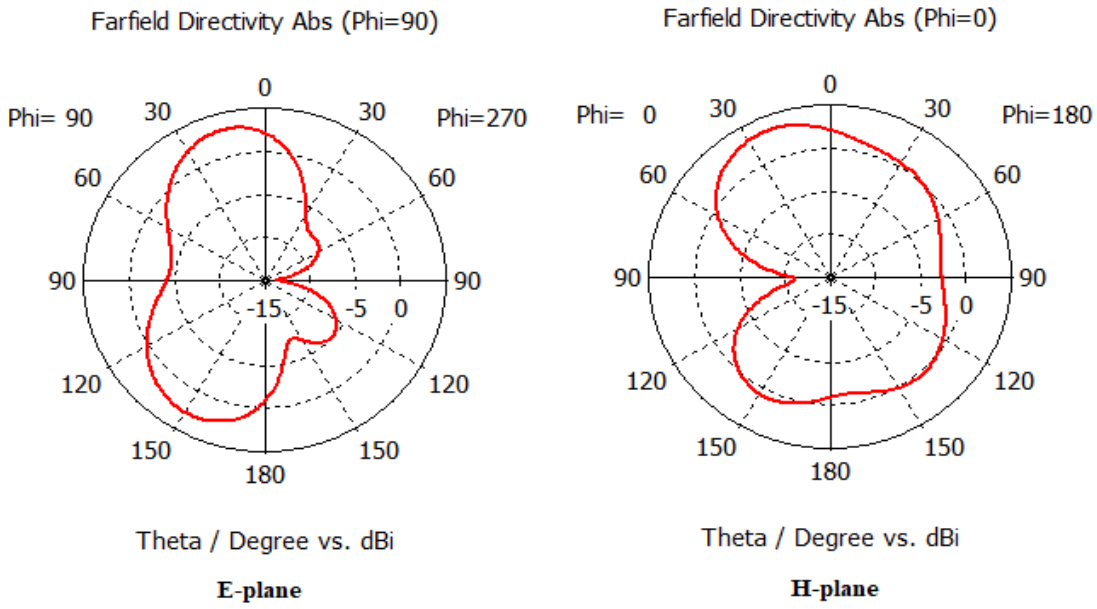

Figure 3.30 Radiation pattern at 6.25 GHz

3.4 Fabrication and Measurement

The proposed structure 8 of the E-shape monopole antenna is fabricated and its input reflection coefficient measured. Figure 3.31 and 3.32 show the photograph of the fabricated antenna and the experimental setup respectively. The simulated and measured reflection coefficient results of the antenna are illustrated in Figure 3.35 where it is observed that the simulated and measured results

are in good agreement. Again, the observed shifts may be attributed to the fact the physical parameters and the geometrical dimensions are not exactly equal to the ones assumed simulation, the fabrication errors and to experimental environment.

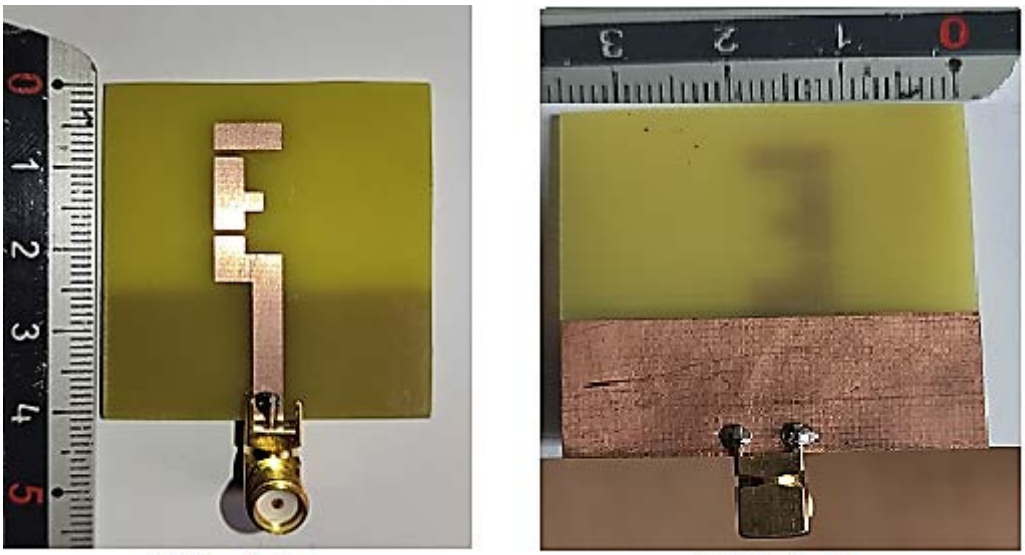

(a) Front view (b) Back view

Figure 3.31 Photograph of the fabricated proposed E-shape antenna prototype

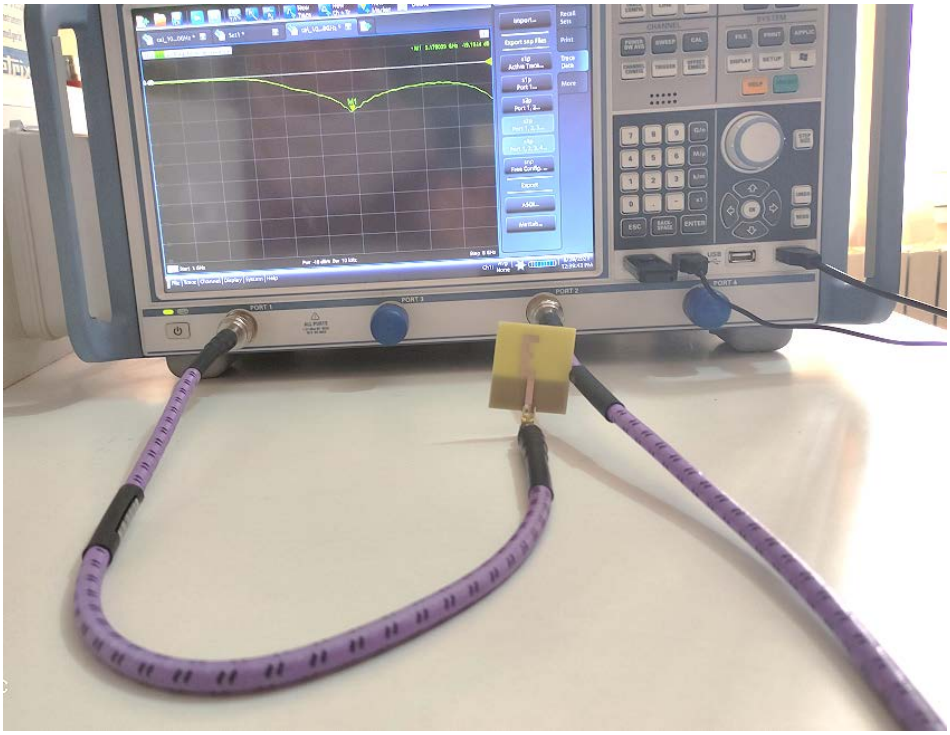

Figure 3.32 Photograph of the experimental setup

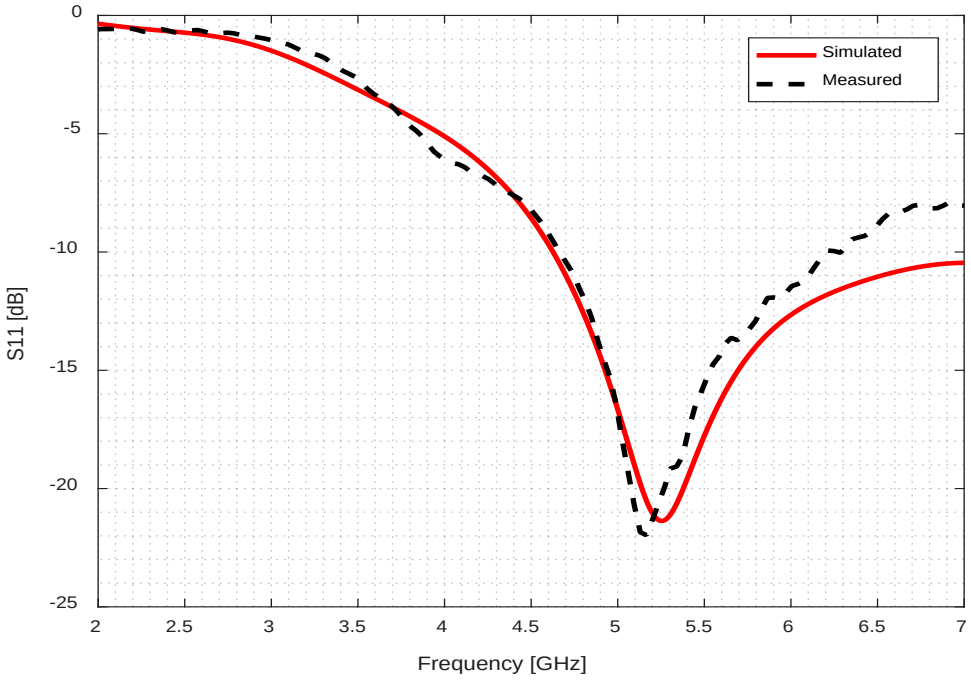

Figure 3.33 Simulated and measured reflection coefficients of proposed antenna

3.5 Conclusion

A parametric analysis has been performed on the previous structure obtained in chapter 2 by changing the slot positions. Nine different antenna configurations have been considered each performing at four (4) modes of operations.

The selected structure 8 operates in one single band and three dual band modes, depending on the state of the switches.

The proposed antenna has been fabricated and its reflection coefficient measured at the first mode where a good agreement between simulated and measured results is observed.

General Conclusion

The objective of this project is the analysis of a planar and frequency reconfigurable E-shape patch antenna using FR-4 substrate.

The analysis started by modification of a published reconfigurable antenna due to difference in its FR-4 substrate physical characteristics and the one at our disposal. Accordingly, appropriate modifications have been performed on the antenna dimensions and on the stripline width so that the modified structure fits the original antenna band characteristics. The antenna operates in two-dual band and two single-band reconfigurable modes, depending on the state of the switches.

In the second part, a parametric analysis of the first structure concerning the slot positions is achieved. The analysis ended up with nine (9) antenna geometrical configurations each one operating in four (4) reconfigurable modes.

One of these antenna configurations -operating in one single-band and three dual band reconfigurable modes- has been considered for further analysis.

The structures fit different applications including Wi-fi, WLAN and Radar.

Prototypes of the modified original antenna as well as the one selected in the second part have been fabricated and their reflection coefficients where measured at the first (OFF, OFF) reconfigurable mode. Good agreements between simulated and measured results have been obtained.

As a further scope, we suggest the following tasks:

- Design and implementation of the switching circuit based on different techniques (PIN diodes, RLC switch)
- Extension of the analysis to other reconfigurable antenna geometries aiming for specified operating frequencies and band characteristics.

References

[1] J.James, P.S. Hall,"Handbook of microstrip antenna", Peter Peregrinus, London, UK, 1989

[2] H.S. Al-Raweshidy and R. Nilavalan "Multi-Band Antenna for Different Wireless Application",2009

[3] Jennifer T. Bernhard "Reconfigurable Antennas",Constantine A. Balanis, Arizona State University

[4] Bernhard, J.T., "Reconfigurable antennas and apertures: State-of-the-art and future outlook," Proceedings of SPIE Conference on Smart Electronics, MEMS, BioMEMS, and Nanotechnology, vol. 5055, pp. 1–9, 2003

[5] S. A. B. A. K. U. A. F. A. T. &. S. B. S. Ullah, «Design and Analysis of a Hexa-Band Frequency Reconfigurable Monopole Antenna,» *IETE Journal of Research,* 2017.

[6] Ramesh Garg, Prakash Bartia, Inder Bahl, Apisak Ittipiboon, "*Microstrip Antenna Design Handbook*'', , pp 1-68, 253-316 , 2001

[7] *"International Journal of Scientific & Engineering Research"*, Volume 5, Issue 3, March-14-1990 ISSN 2229-5518

[8] James j, and P.S. Hall (Eds), *Handbook of microstrip antenna*, Peter Peregrinus, London, UK, 1989

[9] Rahul Rana, and C. Vishnu Vardhana Reddy, "Design of linearly polarized rectangular microstrip patch antenna using IE3D/PSO", National Institute of Technology, Rourkela, 2009.

[10] Constantine, A.balanis," Antenna Theory: Analysis and Design ", 2nd edition, John, Wiley Willey & Sons, Inc, 1997.

[11] Microstrip Antenna Design Handbook – ISBN 0-89006-Garg, Bhartia, Bahl, 2000

[12] D. M. Pozar, "*Microstrip antenna*" proc. IEEE, vol. 80, No, 1 January 1992

[13] [13] Kshetrimayum Milan Singh, Amritesh, "Design of square patch microstrip antenna for circular polarization using IE3D Software", National Institute of Technology, Rourkela.

[14] Broadband Microstrip Antenna –G. Kumar, K. Ray 2003

[15] S. Didouh, M. Abri, and F. T. Bendimerad, "Corporate-Feed Multilayer Bow-Tie Antenna Array Design Using a Simple Transmission Line Model" , Telecommunications Laboratory, Faculty of Technology, Abou-Bekr Belkaid University, 13000 Tlemcen, Algeria.

[16] Prasanna Ramachandran, T.S.Keshav, Laxmikant Minz Vamsikrishna Parupalli and Shaibal

Chakravarty, *''On Antenna Design, Simulation and Fabrication''* PhD Thesis, Deemed University, Nagpur – India 2007

[17] Bahl, I. J and Bhartia, P; “Microstrip Antennas”, Artech House, 1980

[18] Sanchez-Hernandez. *Electrically Small Multiband Antennas, In: Multiband Integrated Antennas for 4G Terminals*, ISBN 9781-59693-331-6, 2008

[19] Mustafa Secmen. *” Multiband and Wideband Antennas for Mobile Communication Systems”*, Recent Developments in Mobile Communications, 2011

[20] Haapala P: Vainikainen, P. and Eratuuli P. *“Dual Frequency Helical Antennas for Handsets”*, IEEE Vehicle Technology Conference, pp. 336-338, ISBN 0-7803-3157-5, April 28-May 1, 1996.

[21] Brown, E.R., “On the gain of a reconfigurable-aperture antenna,” *IEEE Transactions on Antennas and Propagation*, vol. 49, pp. 1357–1362, October 2001. doi:10.1109/8.954923

[22] Bernhard, J.T., “Reconfigurable antennas and apertures: State-of-the-art and future outlook,” Proceedings of SPIE Conference on Smart Electronics, MEMS, BioMEMS, and Nanotechnology, vol. 5055, pp. 1–9, 2003.

[23] Ojaroudi Parchin, N.; Jahanbakhsh Basherlou, H.; Al-Yasir, Y.I.A.; M. Abdulkhaleq, A.; A. Abd-Alhameed, R. Reconfigurable Antennas: Switching Techniques—A Survey. *Electronics* **2020**, *9*, 336. https://doi.org/10.3390/electronics9020336

[24] Clemente, A.; Dussopt, L.; Sauleau, R.; Potier, P.; Pouliguen, P. 1-bit reconfigurable unit cell based on PIN diodes for transmit-array applications in x-band. IEEE Trans. Antennas Propag. **2012**, 60, 2260–2269.